Ecological Modelling 263 (2013) 326–348

Contents lists available at SciVerse ScienceDirect

Ecological Modelling

journal homepage: www.elsevier.com/locate/ecolmodel

Description and validation of production processes in the coral reef ecosystem model CAFFEE (Coral–Algae–Fish-Fisheries Ecosystem Energetics) with a fisheries closure and climatic disturbance

Carlos Ruiz Sebastián[a,b,*], Timothy R. McClanahan[a]

[a] Wildlife Conservation Society, Bronx, NY 10460, USA
[b] Marine Research Institute, University of Cape Town, Rondebosch 7701, South Africa

ARTICLE INFO

Article history:
Received 15 November 2012
Received in revised form 13 May 2013
Accepted 15 May 2013
Available online 22 June 2013

Keywords:
Benthic ecology
Coral reef recovery
Climate change
Marine protected areas
Recovery of fish
Ecosystem models

ABSTRACT

Ecosystem models are well-established tools to investigate the effects of human activities and natural events on marine ecosystems. Recent modeling approaches advocate the integration of physical and biological processes and the coupling of fully-represented ecosystems. Here, we describe a coral reef ecosystem simulation model (CAFFEE) linking reef cover dynamics, benthic and pelagic production and metabolism, detrital pathways and reef formation processes. The model integrates 27 functional groups with coupled two-way trophic and spatial interactions and includes dynamic adjustment of benthic production and consumption processes. The model is validated with a 40 year time series of coral reef field data from Kenyan reefs responding to two disturbances: fisheries closures and a strong thermal anomaly, the 1998 coral bleaching event. The model simulations successfully replicated a number of patterns observed in empirical data, in particular the progression of communities toward greater calcium carbonate deposition following fisheries closure, and the temporal shift to algal-domination after bleaching events. Further validation of the model was garnered from comparisons of emergent model outputs with ecological ratios commonly used to parameterize comparable systems. The model simulations indicate trade-offs among the organic and inorganic (calcium carbonate) processes in coral reefs whereby fisheries closures promote inorganic production and bleaching disturbances favor the organic production processes of the reef.

1. Introduction

Coral reefs are complex ecosystems with an uncertain future (Pandolfi et al., 2011). Their complexity makes it challenging to apply standard empirical scientific principles of ecological investigations using a limited number of controlled components to make holistic predictions about reef responses to common disturbances. Evaluating this complexity requires developing holistic models and running scenarios and testing their results against field studies from similar types of disturbances to validate models, which might then be used to evaluate a larger set of disturbances (Holmes and Johnstone, 2010). The strength of model predictions will depend on the quality of the models and their ability to realistically include key components most influenced by and responding to disturbances. Consequently, testing models under a variety of scenarios is a key step in validating and evaluating their strengths and weaknesses.

Coral reef models have been developed with the purpose of estimating energy flows (Polovina, 1984) and assess a variety of common impacts, including fishing (Arias-González, 1998; Arias-González et al., 2004; Gamble and Link, 2009; Liu et al., 2009; McClanahan, 1992, 1995), eutrophication (Meesters et al., 1998; Wolanski et al., 2004), grazing and sea urchin die-offs (Mumby et al., 2006, 2007), climate change (Baskett et al., 2009, 2010; Crabbe, 2008), and generic or a variety of disturbances (Holmes and Johnstone, 2010; Langmead and Sheppard, 2004). These models differ in their structure and scope and provide useful tests for specific aspects of coral reef ecology and disturbances for specific or regional coral reef systems. As early models have proven to be useful in validating model outputs with field data, efforts to expand their scope remain as a needed next step in investigating model creation and validation (Travers et al., 2007).

Here, we present the overall structure and key processes of one of the larger and more holistic coral reef models and evaluate the benthic and fish components with one of the longer running coral reef monitoring programs (McClanahan, 2008, 2013 in review;

* Corresponding author. Permanent address: 4 Yarrowdale, Pinelands 7405, South Africa. Tel.: +27 216503283; fax: +27 216503283.
E-mail addresses: cruiz@wcs.org, zooxanthelico@gmail.com (C. Ruiz Sebastián), tmcclanahan@wcs.org (T.R. McClanahan).

0304-3800/$ – see front matter © 2013 Elsevier B.V. All rights reserved.
http://dx.doi.org/10.1016/j.ecolmodel.2013.05.012

unpublished data). The purpose is to provide the details needed to understand the model structure, methods of calibration, basic simulation outputs of key components, and test it against an independent empirical time series for a basic set of model scenarios that have parallels in the empirical field data. The scenarios presented here include the recovery of reefs after the closures to fishing and how these reefs responded to a large thermal anomaly or the 1998 bleaching event. These provide the primary ways that the ecological components of the model will be tested and validated before evaluating the fishing components of the model (Ruiz Sebastián and McClanahan, in preparation).

2. Methods

2.1. Conceptual model

The CAFFEE (Coral–Algae–Fish-Fisheries Ecosystem Energetics) model described in this paper simulates the processes driving the biomass and benthic cover dynamics of 27 functional groups representing typical components of coral reef ecosystems in the western Indian Ocean. The trophic interactions between the functional groups (Table s.1 in the supplementary material) are synthesized in a food web (Fig. 1) integrating four types of macrophytes (turf, fleshy and calcifying algae and seagrass), two types of hard corals (branching/foliaceous forms and massive/submassive forms), microplankton, zooplankton, four categories of detrital matter (reef and pelagic particulate and dissolved organic matter), four types of invertebrates (algivores, corallivores, detritivores and micro-invertebrates), and 11 fish guilds (macro- and micro-grazers, scraper-excavators, corallivores, macro- and micro-detritivores, planktivores, macro- and micro-invertivores, piscivores and pisci-invertivores). The model also simulates selective harvesting of fish biomass by five categories of artisanal fisheries common in the region with distinct gear characteristics (fish traps, beach seines, spear guns, gillnets and lines) and associated gear-guild catch ratios. Light and nutrients are the implicit energetic drivers in the model.

CAFFEE simulates the biomass dynamics of the functional groups by time-step computing the energy flows representing metabolic and ecological processes for each biomass pool. The model quantifies the amount of biomass gained as a consequence of production processes, the amount of organic matter used in metabolic maintenance and the organic matter transferred to higher trophic level components due to consumption processes. For autotrophic groups, this can be expressed in terms of biomass-specific rates as:

$$\frac{dB_i}{dt} = B_i \cdot (gp_i - r_i - ep_i - ed_i - ca_i) - \Sigma_j B_j \cdot c_{ij} - \Sigma_k B_i \cdot in_{ik} \quad (1)$$

where dB_i/dt is the rate of change in biomass in the autotrophic group i; gp_i, r_i, ep_i, ed_i are the biomass-specific rates of gross production, respiration, exudation as particulate (POM) and as dissolved organic matter (DOM), respectively, and ca_i is the rate at which energetic resources are used in the deposition of carbonate skeletons by corals and calcifying algae. Consumption of i by grazers or predators j occurs at a rate c_{ij}, while in_{ik} is the rate of biomass loss due to non-trophic interactions with k. All biomass values in the model are referred to in units of mass density (kg wet weight per hectare). For heterotrophic groups, the energetics model can be expressed as:

$$\frac{dB_i}{dt} = (\Sigma_j B_i \cdot c_{ji}) \cdot ae_i \cdot pe_i - B_i \cdot (r_i + m_i) - \Sigma_k B_k \cdot c_{ik} - F_i \quad (2)$$

where dB_i/dt is the rate of change in biomass in consumer group i, B_j is the biomass of prey item j, c_{ji} is the consumption rate of i on prey item j, ae_i and pe_i are the assimilation and production efficiencies of consumer i, r_i and m_i are the respiration and non-predatory mortality rates, c_{ik} is the consumption rate of predator k on i, and F_i is the biomass captured by fisheries. Total biomass consumed by i is $C_i = \Sigma_k B_i \cdot c_{ki}$. Consumer excretion is equivalent to ingested non-assimilated organic matter, therefore $E_i = (1 - ae_i) \cdot C_i$, and is assumed to consist of POM only.

For benthic groups such as macrophytes and corals, biomass cannot be disassociated from the physical space they occupy in the reef. The biomass dynamics of benthic groups are determined by trophic interactions and metabolic processes, both of which are density dependent. In CAFFEE, macrophyte and coral groups are characterized by their biomass and by their occupancy of benthic space, and the ratio between those two state variables provides a measure of biomass density. Occupation of benthic space is a major determinant in benthic productivity and standing stock, thus we have incorporated into CAFFEE the processes driving benthic cover dynamics as conceptualized in Fig. 2. Benthic (planar) cover is described as a percentage of the total benthic space and the cover values of benthic groups are calculated simultaneously to biomass dynamics in time-step calculations with the general form:

$$\frac{dS}{dt} = G + X - C - I \quad (3)$$

where dS/dt is the rate of change in occupied substrate, G and X represent colonization and expansion processes, respectively, and C and I represent the loss of cover due to consumption and non-trophic interactions, respectively. Benthic cover dynamics and their relationships with reef structuring processes are described in detail below.

Conceptually, CAFFEE approach to ecosystem trophodynamic modeling integrates several significant aspects. First, CAFFEE favors modeling of processes based on empirical parameterization of basic metabolism and ecology over derived parameters such as productivity:biomass ratios, consumption:biomass ratios or diet fractions, which in CAFFEE are in fact emerging values rather than forcing values. The use of feedback loops and parameter ranges also favors dynamic self-adjustments to processes and an overall more adaptive modeling approach. Secondly, CAFFEE bioenergetic flows among functional groups are fully coupled, providing a true two-way interaction. Thirdly, detrital pathways are explicitely modeled in CAFFEE, thus providing a critical link between exudation/excretion processes and detritivorous/planktonic consumers and fully accounting for energy and associated pathways. Fourthly, benthic production is biomass-dependent and spatially linked to reef cover dynamics. And fifthly, calcification, erosion and substrate dynamics are explicitely modeled to take into account biotic–abiotic benthic coupling.

2.2. Primary production

2.2.1. Macrophytes

Changes in the biomass of benthic macrophytes result from the balance of gains obtained from gross photosynthetic production and losses due to respiration, exudation as particulate or dissolved organic matter, production of calcium carbonate substrates in the case of calcifying algae, consumption by herbivores and non-trophic interactions with other benthic organisms. Given the assumption of neutral growth at maximum biomass density in the absence of predators and competitors, the relationship between biomass-specific rates for macrophytes in Eq. (1) can be expressed as:

$$gp(\delta) \geq r(\delta) + ep(\delta) + ed(\delta) + ca(\delta) \quad (4)$$

where gross production exceeds respiration, exudation and investment into calcification for any positive value of biomass density (δ) except when at its maximum.

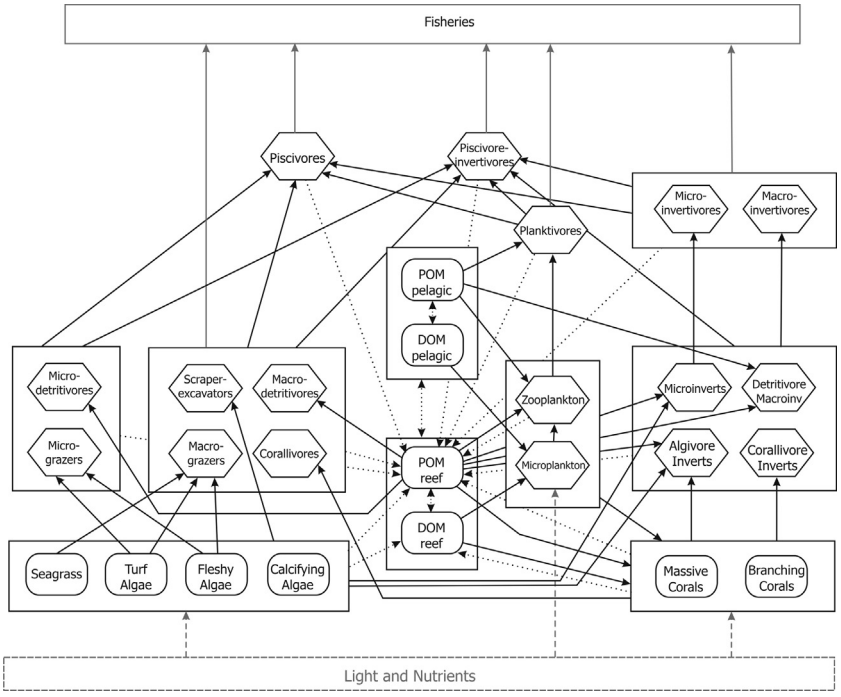

Fig. 1. Food web of a coral reef ecosystem as implemented in CAFFEE, including 27 functional groups and their trophic interactions (solid black arrows). Non-trophic transfers of organic matter (e.g. detrital transfers) are indicated by dotted lines. Extraction of pelagic resources by fisheries is shown in gray solid arrows.

Biomass density of a benthic functional group is defined as the ratio of biomass to occupied surface area, thus:

$$\delta_i = \frac{B_i}{SA_i} \tag{5}$$

where surface area (SA_i) is determined from benthic (planar) cover and topographic complexity and, for corals and calcifying algae, from the surface index (see Section 2.5.2).

The non-linearity of the relationship between production and biomass has been documented for several macrophytes (Copertino et al., 2009; Duarte and Chiscano, 1999; Hackney and Sze, 1988). However, parameterization of production:biomass relationships is complicated because data on algal productivity is more often reported on an aerial than on a biomass basis and biomass density often goes unreported. We have compiled available data on macrophyte energy budgets and derived parameters for biomass density based production, respiration and exudation functions (Eq. (4)) using regression analysis, reported P:R ratios and the assumption of neutral growth at maximum biomass density (Table 1). Our model of benthic macrophytal productivity approximates production and exudation as power functions and respiration as a linear function of biomass density. This production model and the budget balance between curves are based on: (a) maximum net photosynthetic production to biomass ratio decreases with increasing biomass density by a 10-fold factor between maximum and minimum, with an inflexion point near 25% of maximum biomass density (Copertino et al., 2009); (b) respiration rates derived from reported P:R ratios; and (c) excretion as DOM accounts for 30–40% of net production and excretion as POM for a 4–6% of net production. Graphs of the budget curves for each group of macrophytes can be seen in Fig. s.1 in the supplementary material. It should be noted that the set of equations presented represents one of several possible modeling approaches to the empirical data currently available.

2.2.2. Corals

Corals are holobionts in which autotrophic production from symbionts and heterotrophic production from the animal host are

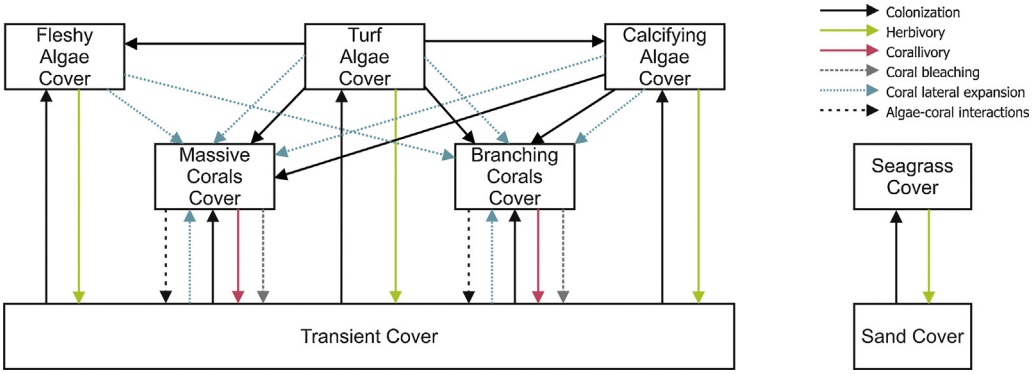

Fig. 2. Benthic space web implemented in the CAFFEE model. Arrows indicate processes driving changes in cover type, with arrowheads pointing in the direction of cover gain. Consumption processes (herbivory, corallivory) result in cover losses for the prey benthic group proportional to the consumed biomass. Colonization by corals of turf or calcifying algae cover (encroachment) similarly results in loss of algae biomass.

Table 1
Parameters of the energy budget of primary producer functional groups in CAFFEE.

Functional group	Parameter	Value	Sources/derivation
Turf algae	Maximum biomass density	$\delta^*_{TA} = 17{,}130\,kg\,ha^{-1}$	McClanahan (1997)
	Gross productivity rate	$gp_{TA}(\delta) = 16.172 \cdot \delta_{TA}^{-0.516}$	Regression analyses based on data in Carpenter (1985) and Copertino et al. (2005)
	Respiration rate	$r_{TA}(\delta) = 0.07154 - 0.00000047 \cdot \delta_{TA}$	
	DOM exudation rate	$ed_{TA}(\delta) = 4.8 \cdot \delta_{TA}^{-0.516}$	Assumes a DOM:Net production ratio of 30–40% based on Abdullah and Fredriksen (2004), Khailov and Burlakova (1969) and Wada et al. (2007), and a POM:Net production ratio of 5–10% based on Ochieng and Erftemeijer (1999) and Wada et al. (2007). Production is balanced by metabolic losses at maximum biomass density (δ^*_{TA})
	POM exudation rate	$ep_{TA}(\delta) = 1.6 \cdot \delta_{TA}^{-0.516}$	
Fleshy and canopy algae	Maximum biomass density	$\delta^*_{FA} = 75{,}000\,kg\,ha^{-1}$	Ateweberhan et al. (2006)
	Gross productivity rate	$gp_{FA}(\delta) = 8 \cdot \delta_{FA}^{-0.516}$	Reports of net production to biomass ratio range from 0.6% to 3.6% (Dhargalkar and Shaikh, 2000; Miller et al., 2009; Penhale and Capone, 1981)
	Respiration rate	$r_{FA}(\delta) = 0.012 + 0.000000016 \cdot \delta_{FA}$	Derived to result in P_g:R values between 2.6 and 5, as reported in Dhargalkar and Shaikh (2000), Miller et al. (2009) and Wanders (1976a,b)
	DOM exudation rate	$ed_{FA}(\delta) = 2.78 \cdot \delta_{FA}^{-0.516}$	See notes on exudation rates in turf algae
	POM exudation rate	$ep_{FA}(\delta) = 0.9 \cdot \delta_{FA}^{-0.516}$	
Calcifying and coralline algae	Maximum biomass density	$\delta^*_{CA} = 4{,}600\,kg\,ha^{-1}$	Ateweberhan et al. (2006)
	Gross productivity rate	$gp_{CA}(\delta) = 3.3 \cdot \delta_{CA}^{-0.516}$	Net production:biomass ratios range from 0.03% to 1% per day but values of ~0.2% are common (Garrigue, 1991; Littler et al., 1986, 1995; Martin et al., 2006)
	Respiration rate	$r_{CA}(\delta) = 0.0203 + 0.00000079 \cdot \delta_{CA}$	Chisholm (2003) reported P_g:R ratios ranging from 1.23 to 2.24 for a range of crustose corallines but higher ratios are often reported (Marsh, 1970; Martin et al., 2006; Wanders, 1976a,b)
	DOM exudation rate	$ed_{CA}(\delta) = 0.7 \cdot \delta_{CA}^{-0.516}$	See notes on exudation rates in turf algae
	POM exudation rate	$ep_{CA}(\delta) = 0.25 \cdot \delta_{CA}^{-0.516}$	
	Cost of calcification rate	$k_{CA}(\delta) = 0.48 \cdot \delta_{CA}^{-0.516}$	Biomass-specific calcification rates derived from Garrigue (1991), Martin et al. (2006), and references therein, commonly lie between 0.01 and 0.04 per day
Seagrass	Maximum biomass density	$\delta^*_{SA} = 61{,}000\,kg\,ha^{-1}$	The maximum biomass density of seagrass reported in the region is 1,070 g (dw) m^{-2} (Bandeira, 2002)
	Gross productivity rate	$gp_{SA}(\delta) = 7.2 \cdot \delta_{SA}^{-0.516}$	Reported net production:biomass ratios are 0.3–3% per day (Bandeira, 2002; Duarte and Chiscano, 1999; Kirsch et al., 2002; Ochieng and Erftemeijer, 1999; van Tussenbroek, 1998)
	Respiration rate	$r_{SA}(\delta) = 0.0205 + 0.00000001 \cdot \delta_{SA}$	Derived to result in P_g:R ratios of 1–1.5 (Ziegler and Benner, 1999)
	DOM exudation rate	$ed_{SA}(\delta) = 0.8 \cdot \delta_{SA}^{-0.516}$	Corresponds to 11% of gross production, in agreement with the findings of Ziegler and Benner (1999)
	POM exudation rate	$ep_{SA}(\delta) = 0.2 \cdot \delta_{SA}^{-0.516}$	3% of gross production and neutral growth at maximum biomass density
Massive and submassive corals	Maximum biomass density	$\delta^*_{MC} = 7{,}500\,kg\,ha^{-1}$	Derived from Fitt et al. (2000) and Anthony et al. (2002)
	Gross productivity rate	$gp_{MC} = 0.007 \cdot \ln(67 \cdot \delta^*_{MC}/\delta_{MC})$	Results in rates ranging from 0.029 to 0.048 d^{-1}. Derived from a reference value of 0.0371 d^{-1} obtained by Anthony and Fabricius (2000) in unshaded *Goniastrea retiformis* colonies in filtered seawater
	Respiration rate	$r_{MC} = 0.0286$	Derived from Anthony and Fabricius (2000). Results in Pg:R ratios of 1.03–1.52. Gross productivity:respiration ratios between 0.97 and 1.35 have been reported by Anthony and Fabricius (2000), Riegl and Branch (1995), Sorokin (1982) and Villinski (2003)
	DOM excretion rate	$ed_{MC} = 0.000889$	Derived from Coffroth (1990) and Riegl and Branch (1995). Assumes that dissolved organic carbon is 70% of total organic carbon (TOC) and that particulate organic carbon (POC) is 30% of TOC, based on Crossland (1987), Nakajima et al. (2009, 2010) and Wild et al. (2004)
	POM excretion rate	$ep_{MC} = 0.000381$	
	Algae-caused mortality rate	$ac_{MC} = 0.0017$	Lirman (2001) reported that corals lose 5–10% of tissue per month due to algal interactions. We have estimated a conservative tissue loss rate of 0.0017 d^{-1}
	Fraction of net growth invested in skeleton	$ca_{MC} = 0.177$	Skeleton growth seems to range from 8% to 22% of tissue growth in massive corals (Anthony et al., 2002) and we have estimated that about 17.7% of net growth is allocated to skeleton growth from the clustering of data points
Branching and foliose corals	Maximum biomass density	$\delta^*_{BC} = 4{,}000\,kg\,ha^{-1}$	Derived from Anthony et al. (2002) and Fitt et al. (2000)
	Gross productivity rate	$gp_{BC} = 0.02 \cdot \ln(10.5 \cdot \delta^*_{BC}/\delta_{BC})$	Results in rates ranging from 0.047 to 0.106 d^{-1}. Derived from a reference value of 0.0792 d^{-1} obtained from an average of rates in Anthony and Fabricius (2000), Falkowski et al. (1984), Gochfeld (1991), McCloskey and Muscatine (1984) and Porter et al. (1984)
	Respiration rate	$r_{BC} = 0.0473$	Derived from respiration rates in *Porites cylindrica* colonies by Anthony and Fabricius (2000). Results in Pg:R ratios of 1.0–1.92. Most reports indicate Pg:R values ranging from 1.18 to 2.20 (Anthony and Fabricius, 2000; Gochfeld, 1991; McCloskey and Muscatine, 1984; Sorokin, 1982)
	DOM excretion rate	$ed_{BC} = 0.0020391$	Derived from Coffroth (1990), Crossland (1987), Muscatine et al. (1984) and Tanaka et al. (2008). Same assumption as for massive corals

Table 1
Parameters of the energy budget of primary producer functional groups in CAFFEE.

Functional group	Parameter	Value	Sources/derivation
	POM excretion rate	$ep_{BC} = 0.0008739$	
	Algae-caused mortality rate	$ac_{BC} = 0.0017$	Lirman (2001) reported that corals lose 5–10% of tissue per month due to algal interactions. We have estimated a conservative tissue loss rate of 0.0017 d^{-1}
	Fraction of net growth invested in skeleton	$ca_{BC} = 0.2857$	According to Anthony et al. (2002) skeleton:tissue growth ratios in branching corals may vary between 10% and 100% and tissue growth may even be negative while skeleton grows. The reasons for this variation are poorly known. We have estimated a 40% skeleton:tissue ratio from the data clustering in Anthony et al. (2002), which results in an investment on skeleton of 28.57% of net growth
Microplankton	Maximum biomass density	$\delta^*_{MP} = 20$ kg ha^{-1} m^{-1} (depth)	From a conservative estimate of phytoplankton biomass of 50 μg C l^{-1} in coastal Kenya by Mutua et al. (2004) and a phytoplankton carbon content of 6% (Opitz, 1996), we estimate a phytoplankton biomass of 8.3 kg (ww) ha^{-1} m^{-1}, and a maximum microplankton (including benthoplankton) biomass of 20 kg ha^{-1} m^{-1}

the energy inputs balanced by the losses of the whole organism. Consequently, the energy budget for corals combines Eq. (1) with a heterotrophic contribution based on consumption of plankton and detritus, and is expressed as:

$$\frac{dB_i}{dt} = [B_i \cdot (gp_i - r_i - ep_i - ed_i - ac_i) + ae_i \cdot pe_i \cdot \Sigma_j B_i \cdot c_{ji}] \cdot (1 - ca_i) - \Sigma_k B_k \cdot c_{ik} \quad (6)$$

where all terms have been previously described except for ac_i which is the rate of biomass loss caused by macro–algae interactions (Lirman, 2001). The assimilation (ae) and production (pe) efficiencies of corals and other consumer groups are summarized in Table s.2 in the supplementary material.

Photosynthetic production in corals is strongly influenced by light availability and, to a lesser extent, by POM concentration (Anthony and Fabricius, 2000), and the rates of auto- and heterotrophic production may not be independent (Anthony and Fabricius, 2000). As previously done for production of macrophytes, we constructed coral autotrophic production curves based on reported gross productivity values, productivity:respiration ratios and mucus excretion rates. We also assumed that coral photosynthetic production rate has a logarithmic relationship with biomass density and results in neutral growth at maximum biomass. Evidence suggesting that the relationship between coral photosynthetic production rate and coral biomass may be logarithmic was reported by McCloskey and Muscatine (1984). Respiration, excretion and calcification processes have been modeled as linearly related to biomass density, which would explain the variability observed in gross productivity:respiration ratios seen in the literature. Ratios of tissue growth:skeleton growth and energetic investment into tissue and skeletal growth show considerable variation with colony size and morphology, light and heterotrophy (Anthony et al., 2002; Ferrier-Pagès et al., 2003) but, for simplicity, we have modeled coral investment into calcification as a fixed fraction of net growth. The parameterization of Eq. (6) for the two coral functional groups is summarized in Table 1 and graphs of the energy budget curves for corals can be seen in Fig. s.2 in the supplementary material.

2.2.3. Autotrophic plankton

Microplankton, including bacterio- and phytoplankton, planktonic protozoa and metazoan larvae, constitute the microbial component of the reef food web, with the autotrophic components making a substantial contribution to reefal primary production (Sorokin and Sorokin, 2009). Microbial food webs are notoriously difficult to integrate in ecosystem models due to the phylogenetic, trophic, metabolic and size diversity of their constituent organisms, and the challenge of deriving energy budgets for individual components in an ecosystem-level dynamic system is further complicated given the differences between relevant time scales for these low-biomass high-turnover pools. We have simplified this complexity by pooling all bacterio-, pico-, nano- and phytoplanktonic organisms into a single functional group (Microplankton) characterized mainly as a primary producer, but also removing dissolved organic carbon (DOC) from the system by consumption processes. Pooling of organisms with different trophism in a functional group and within-group trophic transfer could potentially lead to overstated productivity, therefore calibration in this group seems particularly sensitive.

Given that the auto- and heterotrophic components in microplankton have daily doubling rates ranging from 0.8 to 4, and from 1.1 to 2.9, respectively (Pomeroy et al., 1995; Ferrier-Pagès and Gattuso, 1998) and that an undetermined portion of the autotrophic production of microplankton is consumed by its heterotrophic components, we have estimated an overall daily maximum biomass-specific net production rate of 4 for the microplankton biomass pool. Furthermore, we have estimated a maximum microplankton biomass of 20 kg ha^{-1} per meter of water column (Table 1) and modeled net productivity of microplankton using a sigmoidal curve with the equation:

$$np_{MP} = \frac{4}{\left(1 + 10^{0.2(B_{MP}/rd)-2}\right)} \quad (7)$$

where B_{MP} is the biomass of microplankton and rd is the reef depth (in meters). Graphs of net productivity of microplankton can be found in Fig. s.3 in the supplementary material.

2.3. Consumption and metabolic processes

2.3.1. Consumption

Fish, invertebrates and zooplankton entirely satisfy their energy requirements through consumption processes, whereas heterotrophy plays a more complex role in corals (Anthony and Fabricius, 2000; Grottoli et al., 2006). Consumers acquire their energetic resources at a consumption rate (ce, the fraction of consumer biomass equivalent to daily ingested prey biomass) which we have defined as a function of the ratio between prey biomass and predators and competitors biomass. Predator–prey theory has predominantly held the view that the functional response of predators is mainly driven by prey density, but this view has been challenged by suggestions that ratio-dependent functional responses (i.e. dependent on the ratio between prey and predators) in predator–prey models may represent population dynamics more accurately than prey-density models, especially in heterogeneous

environments (Akçakaya et al., 1995; Arditi and Ginzburg, 1989; Arditi and Saïah, 1992; Berryman, 1992; Berryman et al., 1995; Ginzburg and Akçakaya, 1992). Nevertheless, functional responses may well encompass a spectrum of perception in which density of predators, prey and co-habitating populations may all be relevant factors (Abrams and Ginzburg, 2000; Schenk et al., 2005). The role of competition in modulating the functional response is receiving increasing attention in fisheries and ecological models (de Villemereuil and López-Sepulcre, 2011; Gamble and Link, 2009). In our model, we consider the functional response of predators (consumers) as a function of a food-to-consumers ratio (θ) that includes resource and interference competition. Thus, for consumer j this ratio is expressed as:

$$\theta_j = \frac{\Sigma_i B_i}{B_j + \Sigma_k B_k \cdot cc_{kj}} \tag{8}$$

where B_i is the biomass of prey item i, B_j is the biomass of consumer j, B_k is the biomass of competitor group k and cc_{kj} is a competition coefficient of k on j. Thus the food-to-consumers ratio is a prey-predator biomass ratio weighted by competition. Given this food-to-consumers ratio, we define the biomass-specific consumption rate of consumer j, $ce(\theta_j)$, as following a sigmoidal model expressed as:

$$ce(\theta_j) = \frac{ce_j^{\max}}{1 + 10^{\left(\theta_j^{\mathrm{mid}} - \theta_j\right) \cdot \theta_j^{sl}}} \tag{9}$$

where $ce_j^{\max}$ is the estimated maximum consumption rate of j, and θ_j^{mid} and θ_j^{sl} are the midpoint and slope, respectively, of the sigmoidal function (Fig. 3). Type III or sigmoidal functional response models often show the best fit to empirical data (Aljetlawi et al., 2004; Eggleston et al., 1992; Englund and Leonardsson, 2008; Piana et al., 2006; Viherluoto and Viitasalo, 2001). Consumption parameters have been summarized in Table s.3 in the supplementary material. Estimates of consumption rates were derived from the literature and adjusted during model calibration.

Given that ce is a biomass-specific consumption rate, we can express the total amount of prey biomass ingested by consumer j as $C_j = B_j \cdot ce(\theta_j)$ or, assuming that j consumes prey items proportionally to their biomass relative to total prey biomass, as:

$$C_j = \Sigma_k B_j \cdot ce(\theta_j) \cdot \frac{B_k}{\Sigma_p B_p} \tag{10}$$

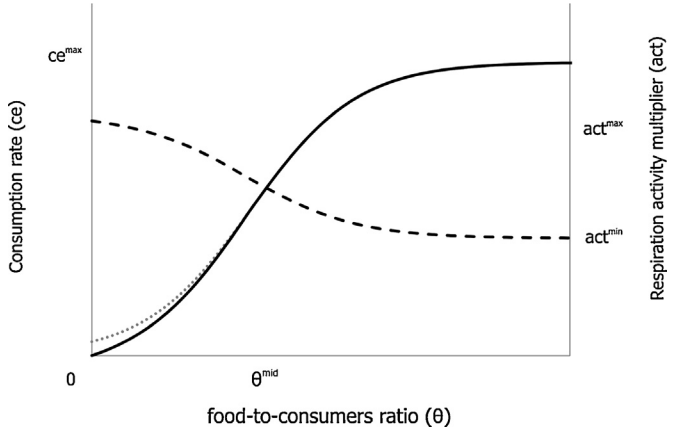

Fig. 3. Consumption and respiration rates in CAFFEE as functions of a food-to-consumers ratio. The consumption rate sigmoid curve (solid line) approaches maximum consumption rate ($ce^{\max}$) as the food-to-consumers ratio reaches food saturation level (at θ^{mid} times 2). The respiration activity multiplier (dashed line) ranges from its maximum value ($act^{\max}$) at low θ values to its minimum value ($act^{\min}$) at food saturation level. The consumption rate was forced through the origin by proportionally adjusting the original sigmoidal curve (dotted line).

where the last term is the diet portion of prey item k in the consumption of j. Thus, prey-predator consumption rates can be expressed as $c_{kj} = ce(\theta_j) \cdot (B_k / \Sigma_p B_p)$. Dynamic adjustment of diet portions based on relative biomass is one way of simulating prey-switching, a feedback mechanism often associated with sigmoid functional responses. However, biomass-proportionality is only one of multiple hypotheses upon which to build a consumption model. Alternative or complementary hypotheses may consider predator dietary preferences, prey vulnerability factors such as individual prey size, or environmental effects such as refuge availability. We chose to introduce a "preyability" index (υ_{ij}, preyability of prey item i by predator j) in predator–prey interactions that encapsulates different factors affecting predator catch rates on particular prey. The effect of this preyability index is to weight the proportional-biomass diet portion thus transforming Eqs. (8) and (10) into:

$$\theta_j = \frac{\Sigma_i B_i \cdot \upsilon_{ij}}{B_j + \Sigma_k B_k \cdot cc_{kj}}, \quad \text{and} \tag{11}$$

$$C_j = \Sigma_k B_j \cdot ce(\theta_j) \cdot \frac{\upsilon_{kj} \cdot B_k}{\Sigma_p \upsilon_{pj} \cdot B_p} \tag{12}$$

The preyability indices and competition coefficients values used in the present simulations have been summarized in Table s.3 in the supplementary material.

2.3.2. Coral heterotrophy

The relative contribution of heterotrophy to coral energetic budgets has long been subject to debate. Corals consume zooplankton, microplankton, POM, and DOM (Houlbrèque and Ferrier-Pagès, 2009; Sorokin, 1982) at rates that are influenced by prey concentration (Anthony and Fabricius, 2000; Ferrier-Pagès et al., 2003; Palardy et al., 2006), colony size (Kim and Lasker, 1998), luminosity (Anthony and Fabricius, 2000; Ferrier-Pagès et al., 2003) and symbiont concentration (Grottoli et al., 2006; Palardy et al., 2008), among other factors.

Coral heterotrophy differs from other consumption processes in important aspects that justify modifications to the consumption model presented above. As passive consumers, distinct consumption rates for each prey type have been considered to be independent from the total amount of prey, but proportional to the concentration of each particular prey type (Ferrier-Pagès et al., 2003; Houlbrèque et al., 2004; Palardy et al., 2006) and to follow a type-II functional response (Anthony and Connolly, 2004). Because surface area of the consumer, not biomass, is directly related to consumption rate and heterotrophy rates decrease with increasing colony size (Kim and Lasker, 1998), we have introduced an allometric correction factor in the calculations of coral consumption. The amount of zooplankton, microplankton, reef POM and reef DOM captured by corals is thus described by the equation:

$$C_j = \Sigma_k B_j \cdot ce(\theta_j)_k \cdot (1 - 1.12 \cdot \log_{10} \sigma_j), \tag{13}$$

where C_j is the total biomass consumed by coral group j, k is a particular coral prey type, $ce(\theta_j)_k$ is the consumption rate of k by j, and σ_j is the surface index of coral j (see Section 2.5.2). The logarythmic allometric correction factor was empirically estimated from model simulation runs.

2.3.3. Microplankton consumption

Heterotrophic production by microplankton was integrated with autotrophic production in a net production rate described in Section 2.2.3. However, this mechanism also requires the removal of DOM from the reef and pelagic pools for the budget balance of these detrital pools. Bacterioplankton are the major contributors to the remineralisation of DOM of benthic origin, removing more

than 50% of the DOC released (Ziegler and Benner, 1999). Consumption dynamics are complex due to differences in lability of the available organic matter, but the uptake rates of highly labile algal exudates are in the order of 1.5 times the microbial biomass per day (Pett, 1989). Given that our microplankton functional group includes more than just bacterioplankton, we have conservatively estimated a constant biomass-specific consumption rate of DOM by microplankton of 0.5 per day.

2.3.4. Respiration and non-predatory mortality

The respiration rate of consumers (r in Eq. (2)) is parameterized as a biomass-specific basal (or standard) respiration rate (ρ) multiplied by an activity factor representing the increase in metabolic expenditure due to consumer motion and activity. Bioenergetics fish population models suggest that activity may represent a large and variable fraction of energy budgets (Boisclair and Legget, 1989) where multiple factors, mostly poorly known, are involved (Boisclair, 2001; Chipps and Wahl, 2008). Recent studies have linked activity levels in fish to prey diversity, abundance, size and morphology (Sogard and Olla, 1996; Chipps and Wahl, 2008, and references therein). Based on the assumption that food scarcity increases foraging activity, we have modeled the activity factor as a sigmoid function of the food-to-consumers ratio (θ) between minimum and maximum activity values (Fig. 3). The activity factor of consumer j can then be expressed as:

$$\mathrm{act}(\theta_j) = \mathrm{act}_j^{\min} + \frac{\mathrm{act}_j^{\max} - \mathrm{act}_j^{\min}}{1 + 10^{(\theta_j - \theta_j^{\mathrm{mid}}) \cdot \theta_j^{\mathrm{sl}}}} \tag{14}$$

where $\mathrm{act}_j^{\max}$ and $\mathrm{act}_j^{\min}$ are the maximum and minimum values of the activity multiplier for consumer j, respectively. Respiration rates are then expressed as:

$$r_j = \rho_j \cdot \mathrm{act}(\theta_j) \tag{15}$$

Basal respiration rates and maximum and minimum activity factors for functional groups have been summarized in Table s.4 in the supplementary material.

Mortality due to causes other than predation is generally difficult to estimate from field data, although it is often used as a limiting parameter for population growth (e.g. Carpenter et al., 1994). We have parameterized non-predatory mortality (m in Eq. (2)) as a biomass-specific rate formulated as a linear function of biomass density, expressed as:

$$m_j = \mu_j \cdot B_j, \tag{16}$$

where μ_j is the non-predatory mortality (NPM) coefficient of group j. Estimates for NPM coefficients were derived heuristically from model simulation runs during calibration and have been included in Table s.4 in the supplementary material. The amount of biomass lost to NPM for group j can thus be expressed as:

$$M_j = B_j \cdot m_j \tag{17}$$

2.4. Detrital pathways

Detrital organic matter is represented in CAFFEE by four biomass pools: reef POM, reef DOM, pelagic POM and pelagic DOM. The processes driving the dynamics of the detrital biomass pools are conceptualized in Fig. 4. The organic portion of macrophyte particulate exudates and animal excreta and carcasses enter the reef POM pool, where it is consumed by detritivores, transported to the pelagic POM pool, buried into sediment, or degraded into reef DOM as a consequence of passive leakage. Macrophyte and coral DOM exudates enter the reef DOM pool after elimination of the refractory fraction, where they are consumed by microplankton and corals, degraded by photoreactivity and diagenetic processes, or transported to pelagic DOM. Pelagic POM and DOM are consumed by their respective levels of detritivores, or further transported to adjacent offshore or onshore systems. For simplicity, we have assumed that biomass enters the detrital pools only at the reef level and that there is a net flux of biomass between reef and pelagic pools, albeit a more accurate representation would take into account turbulence and flow dynamics. A fraction of the biomass entering the pools consists of inorganic materials and refractory organic matter and this is therefore not incorporated into the energetic cycle and thus abandons the system, while the remaining labile fraction is recycled.

Photodegradation due to exposure to UV radiation and loss of bioreactivity due to diagenetic processes are the main causes of DOM degradation. We have estimated a biomass-specific DOM degradation rate (ϑ) of 0.5 d^{-1} based on Amon and Benner (1996), Pausz and Herndl (1999), Tranvik and Kokalj (1998) and Wada et al. (2008). The budget equations for the detrital biomass pools are:

$$\frac{dB_{r\mathrm{POM}}}{dt} = \Sigma_i \lambda_i \cdot (Ep_i + M_i) - \Sigma_j C_j - (\tau_{r\mathrm{POM}\to r\mathrm{DOM}} + \tau_{r\mathrm{POM}\to p\mathrm{POM}}) \cdot B_{r\mathrm{POM}} - \xi_{r\mathrm{POM}\to\mathrm{sed}} \cdot S_{\mathrm{sand}} \tag{18}$$

$$\frac{dB_{r\mathrm{DOM}}}{dt} = \Sigma_i \Lambda_i \cdot Ed_i + \tau_{r\mathrm{POM}\to r\mathrm{DOM}} \cdot B_{r\mathrm{POM}} - \Sigma_j C_j - (\vartheta + \tau_{r\mathrm{DOM}\to p\mathrm{DOM}}) \cdot B_{r\mathrm{DOM}} \tag{19}$$

$$\frac{dB_{p\mathrm{POM}}}{dt} = \tau_{r\mathrm{POM}\to p\mathrm{POM}} \cdot B_{r\mathrm{POM}} - \Sigma_j C_j - (\tau_{p\mathrm{POM}\to p\mathrm{DOM}} + \xi_{p\mathrm{POM}\to\mathrm{off}} + \xi_{p\mathrm{POM}\to\mathrm{on}}) \cdot B_{p\mathrm{POM}} \tag{20}$$

$$\frac{dB_{p\mathrm{DOM}}}{dt} = \tau_{r\mathrm{DOM}\to p\mathrm{DOM}} \cdot B_{r\mathrm{DOM}} + \tau_{p\mathrm{POM}\to p\mathrm{DOM}} \cdot B_{p\mathrm{POM}} - \Sigma_j C_j - (\vartheta + \xi_{p\mathrm{DOM}\to\mathrm{off}}) \cdot B_{p\mathrm{DOM}} \tag{21}$$

where dB_k/dt is the rate of change of each detrital biomass pool, λ_i and Λ_i are the organic and labile fractions of POM and DOM, respectively, of excreta of diverse origin (Table s.5 in the supplementary material), Ep_i and Ed_i are the biomass excreted or exudated as POM and DOM, respectively, and M_i is the biomass input from non-predatory mortality (Eq. (17)). POM or DOM consumed is denoted as $\Sigma_j C_j$. Rates of transport between detrital compartments (τ) and exports to adjacent systems (ξ) are summarized in Table s.6 in the supplementary material.

2.5. Reef formation processes

2.5.1. Skeletal structures and reef framework

Calcium carbonate is deposited by corals and calcifying algae as structural support for growth. The dynamics of these skeletal structures are mainly driven by the processes of calcification, erosion (biological, physical and chemical) and mortality. Calcification increases the standing stock of the skeletons of living coral and calcifying algae, whereas erosion and mortality reduce those stocks, incorporating its constituents into the reef framework as dead coral, rubble, or sand. Coral mortality, as a consequence of predation, disease, algal allelopathy or bleaching, results in the exposed coral skeleton becoming part of the reef framework. The reef framework itself is subject to erosion by eroding agents. Conceptually, the dynamic budgets of coral or algae skeleton (K_i) and reef framework (W) can be expressed as:

$$\frac{dK}{dt} = \mathrm{PK} - \mathrm{EK} - \mathrm{LK}, \tag{22}$$

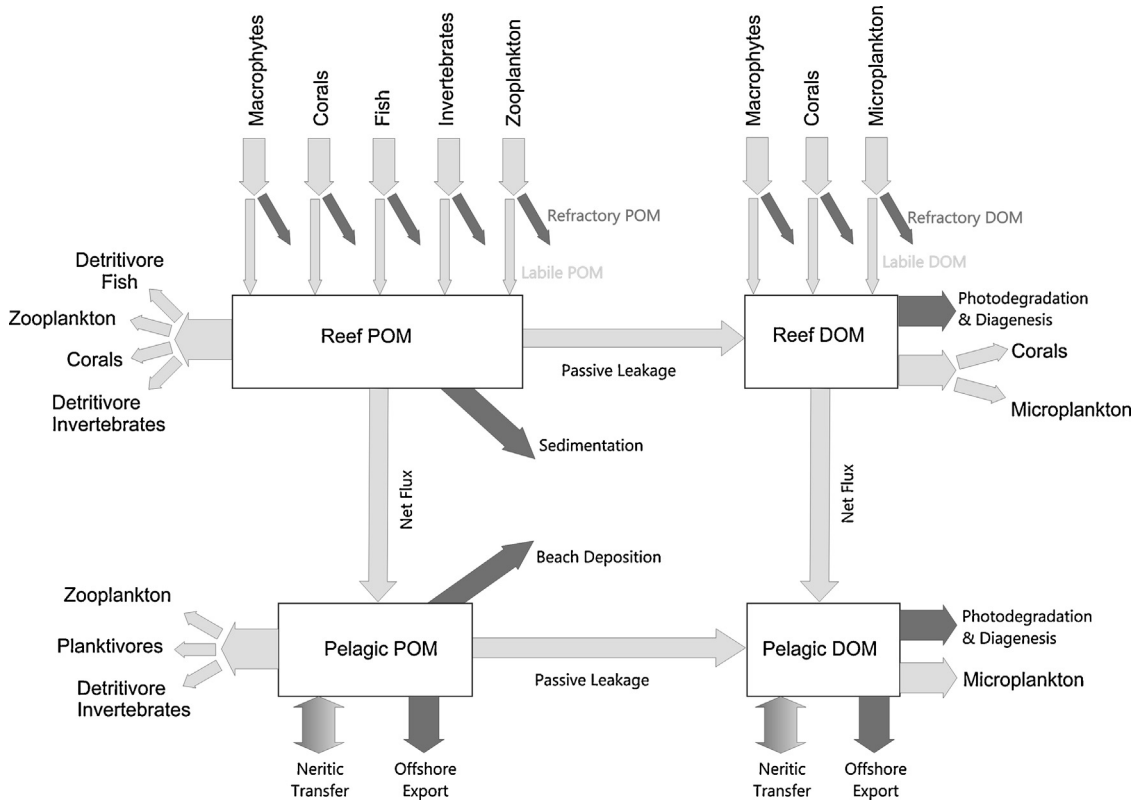

Fig. 4. Detrital pathways in CAFFEE representing a simplified model of the transference and transformation of particulate and dissolved organic matter in a coral reef ecosystem. Detrital matter exiting the system is indicated by dark arrows.

where PK is the skeleton produced, EK is the skeleton loss caused by erosion, and LK is the amount of skeleton transferred to the framework as a consequence of predation, bleaching or interactions; and

$$\frac{dW}{dt} = \mathrm{LK} - \mathrm{EW} \tag{23}$$

where EW represents erosion processes on framework structure.

The amount of skeleton produced can be derived from the energetic investment into calcification (ca_i) in Eqs. (1) and (6). Thus, for calcifying algae, this is:

$$\mathrm{PK_{CA}} = B_{\mathrm{CA}} \cdot ca_{\mathrm{CA}} \cdot \kappa_{\mathrm{CA}}, \tag{24}$$

and for corals:

$$\mathrm{PK}_i = [B_i \cdot (gp_i - r_i - ep_i - ed_i - ac_i) + ae_i \cdot pe_i \cdot \Sigma_j B_i \cdot c_{ji}] \cdot ca_i \cdot \kappa_i \tag{25}$$

where all the terms have been previously described except for the κ coefficients, which are conversion factors between biomass invested in calcification and amount of calcium carbonate mass deposited. Given a coral tissue enthalpy of 29.4 J mg^{-1}, a $CaCO_3$ deposition cost in corals of 0.152 J mg^{-1} $CaCO_3$, and a metabolic conversion efficiency of 0.75 (Anthony et al., 2002), the value of κ for corals is 32.93 mg $CaCO_3$ mg^{-1} coral tissue. Given that the calorific value of calcifying algae tissue is approximately one tenth that of coral tissue (Paine and Vadas, 1969; Littler and Kauker, 1984) we have estimated κ_{CA} as 10% of the conversion factor for corals.

Biological reef eroders include parrotfishes, sea urchins, boring sponges, polychaete worms, mollusks and others (Glynn, 1996) but only the former two are significant bioeroders in Kenyan reefs (Carreiro-Silva and McClanahan, 2001). Erosion of live coral skeleton by parrotfishes and corallivorous fish is low (Glynn, 1996; Jayewardene and Birkeland, 2006; Jayewardene et al., 2009) but the eroding effect by parrotfishes on reef framework is of some consideration (Alwany et al., 2009; Bellwood, 1995; Bruggemann et al., 1996; Hoey and Bellwood, 2008). The erosion rate of scarids on reef framework ($\varepsilon_{\mathrm{SC}}$) depends heavily on their feeding mode (i.e. scrapers versus excavators) (Alwany et al., 2009; Hoey and Bellwood, 2008) and we have estimated an overall daily rate of 1 g $CaCO_3$ ingested per g fish biomass (Hoey and Bellwood, 2008). Sea urchins have lower rates of bioerosion on reef framework (0.004–0.023 g $CaCO_3$ g ww d^{-1}) but can have a major effect at high abundance (Brown-Saracino et al., 2007; Carreiro-Silva and McClanahan, 2001). Based on results obtained in Kenyan reefs, we have estimated a daily erosion rate of urchins on reef framework ($\varepsilon_{\mathrm{AI}}$) of 0.011 g $CaCO_3$ g^{-1} ww urchin and proportional to exposed framework. Thus, we have parameterized the bioerosion terms in Eqs. (22) and (23) as:

$$\mathrm{EK}_i = \Sigma_j C_{ij} \cdot \gamma_{ij}, \tag{26}$$

where C_{ij} is the consumption of i by j, and γ_{ij} is a coefficient of bioerosion proportionality between biomass consumed and eroded skeleton (Table s.7 in the supplementary material); and:

$$\mathrm{EW} = (B_{\mathrm{SC}} \cdot \varepsilon_{\mathrm{SC}} + B_{\mathrm{AI}} \cdot \varepsilon_{\mathrm{AI}}) \cdot (S_{\mathrm{T}} + S_{\mathrm{TA}}), \tag{27}$$

where B_{SC}, B_{AI}, $\varepsilon_{\mathrm{SC}}$ and $\varepsilon_{\mathrm{AI}}$ are the biomass and biomass-specific erosion rates of scraper-excavator fish and algivore invertebrates, respectively, and S_{T} and S_{TA} are the benthic cover of exposed reef framework (transient cover) and turf algae, respectively.

Herbivory on calcifying algae and corallivory, while generally having little effect on skeletal erosion, provide clear substrates for colonization by benthic organisms (Bellwood, 1995; Bruggemann et al., 1996) and contribute to benthic space dynamics by transferring the exposed substrate to the reef framework, as do other processes such as coral mortality due to algal interactions, bleaching or disease. To quantify the amount of skeleton loss caused by

mortality and consumption processes we define the coefficient β (cover reduction ratio) as the fraction of lost biomass that results in loss of benthic cover. We have estimated cover reduction ratio values of 0.08, 0.03, 0.07 and 0.03 for herbivory on turf, fleshy, calcifying algae and seagrass, respectively, and a value of 0.01 for corallivory. Thus, the skeleton loss due to consumption and mortality (LK in Eqs. (22) and (23)) can be expressed as:

$$\mathrm{LK}_i = \frac{(C_i + I_i)\cdot \beta_i}{\delta_i} \cdot \frac{K_i}{\sigma_i \cdot S_i}, \tag{28}$$

where C_i and I_i are the amounts of biomass lost to consumption and non-trophic interactions, respectively, β_i is the cover reduction ratio and δ_i is the biomass density. Therefore the first term in Eq. (28) represents the amount of lost benthic surface area and the second term is used to normalize lost benthic space to planar area and calculate the amount of skeleton in the lost area. K_i, σ_i and S_i are skeleton mass, surface index and benthic space, respectively.

2.5.2. Reef topography

Reef topography exerts a substantial influence on benthic processes as it affects the amount of physical space available to sessile organisms and therefore benthic productivity, and its influence extends to pelagic reef inhabitants though trophic cascades and habitat heterogeneity. Measurements of reef topography in field studies are usually recorded as reef rugosity, a measure of the ratio between three-dimensional and planar surface area in reefs, with values usually ranging between ~1 and 2 worldwide (Holmes, 2008) and between 1.12 and 1.5 in the western Indian Ocean (Garpe and Öhman, 2003; McClanahan, 1994). However, the techniques used in measurements of reef rugosity do not differentiate between benthic complexity due to reef framework topography and rugosity due to the supporting structures of live organisms. This distinction merits consideration in a process-based model as both levels of benthic complexity exert their influence on different processes. We define framework complexity (ω) as the ratio between the three-dimensional and planar surface area of the reef framework, and surface index (σ) as the ratio between the three-dimensional and planar surface area of calcifying benthic organisms. Framework complexity affects mainly the dynamics of benthic space, whereas surface indices play a more important role in the energy budgets of benthic groups, particularly on corals.

The surface area (SA_i in Eq. (5)) occupied by benthic groups is calculated from the product of planar space, reef framework complexity and surface index, as:

$$SA_i = S_i \cdot \omega \cdot \sigma_i \tag{29}$$

Holmes (2008) estimated the surface index of massive and submassive corals as 3.2 and 5.9, respectively, and that of branching and foliose forms as 6.3 and 3, respectively. In order to reflect changes in surface index with skeleton dynamics, we have parameterized σ as a function of skeleton mass, as follows:

$$\sigma_{\mathrm{MC}} = 0.8 + \frac{3}{1 + 10^{(1.05 - 0.000021 \cdot K_{\mathrm{MC}})}}, \quad \text{and} \tag{30}$$

$$\sigma_{\mathrm{BC}} = 0.8 + \frac{3.5}{1 + 10^{(1 - 0.000025 \cdot K_{\mathrm{BC}})}} \tag{31}$$

for massive and branching corals respectively. We have calibrated these curves based on ellipsoid geometry and an average mass density of coral skeleton of 1.5 g cm^{-3} for massive corals (see Fig. s.4 in the supplementary material for more details). The surface index in turf and fleshy algae cover is considered to be 1, as is for calcifying algae, for which we have assumed that the increase in surface area due to skeletal structure does not enhance significantly the effect of reef framework complexity. Given that skeletal growth in corals overlaps framework complexity, the cumulative factoring of ω and σ in corals may lead to overestimating surface area; we have compensated for this effect by using lower maxima surface index values (3.8 for massive and 4.3 for branching corals) with respect to those reported by Holmes (2008). The relationship between mass of reef framework (W) and reef framework complexity (ω) is difficult to ascertain and we have assumed a general value of ω = 1.3 for western Indian Ocean reefs (Garpe and Öhman, 2003; McClanahan, 1994) regardless of framework dynamics.

2.6. Reef substrate dynamics

Reef benthic space is a critical resource for sessile organisms and a determinant factor in the standing stock and productivity of macrophytes and corals. Benthic cover dynamics were briefly introduced above with reference to Fig. 2 and described in Eq. (3). In our model, benthic cover is the basic currency of spatial area for benthic organisms and its unit is a fraction of the total area represented by the model virtual space. For simplicity, we make an explicit distinction between sandy and hard substrates in the reef, with sand cover being exclusively available to seagrass while hard substrate can only be occupied by the other benthic groups. No explicit processes have been modeled to simulate the dynamics between sand cover and hard substrates.

The basic processes driving benthic cover dynamics are cover gains due to recruitment (either on transient reef space or into already occupied but suitable settlement space, i.e. encroachment) and lateral expansion (or overgrowth), and cover losses due to extirpation (during herbivory and corallivory) and interactions (such as algal allelopathy). This was introduced earlier (Eq. (3)) and these processes can be parameterized as:

$$\frac{dS_i}{dt} = \Sigma_j(S_j \cdot g_{ij} + SE_{ij}) - \frac{\beta_i}{\sigma_i \cdot \delta_i} \cdot (\Sigma_k B_k \cdot c_{ik} + \Sigma_l B_i \cdot in_{il}) \tag{32}$$

where dS_i/dt is the change in benthic cover in benthic group i, S_j is the benthic cover of group j, g_{ij} is the recruitment rate of benthic group i on group j (Table s.8 in the supplementary material), SE_{ij} is the space gained by overgrowth of i on j due to lateral expansion, β_i is the corresponding cover reduction ratio, σ_i is the surface index of i and δ_i is the biomass density of i. The last two terms in Eq. (32) correspond to the biomass of i lost due to consumption and non-trophic interactions, respectively. Recruitment rates in corals are linearly correlated with free space and unrelated to coral cover (Connell et al., 1997).

Coral lateral growth results in cover gains at the expense of transient or algal cover (coral–coral overgrowth is assumed to be neutral for simplicity). Lateral extension of coral colonies is a consequence of the calcification process whereby calcium carbonate is deposited at the growing edges of the coral colony. Thus, the amount of deposited carbonate that actually results in a gain in benthic cover space is only a relatively small fraction of the total carbonate skeleton deposited. In massive corals, this is limited to the new skeleton deposited in the outer margin at the base of the colony; in branching corals, in addition, it includes the lateral growth in peripheral branches overgrowing other substrata. We have parameterized benthic space gained due to lateral expansion as:

$$\mathrm{SE}_i = \frac{\mathrm{PK}_i}{SA_i \cdot kd_i} \cdot la_i \cdot cor, \tag{33}$$

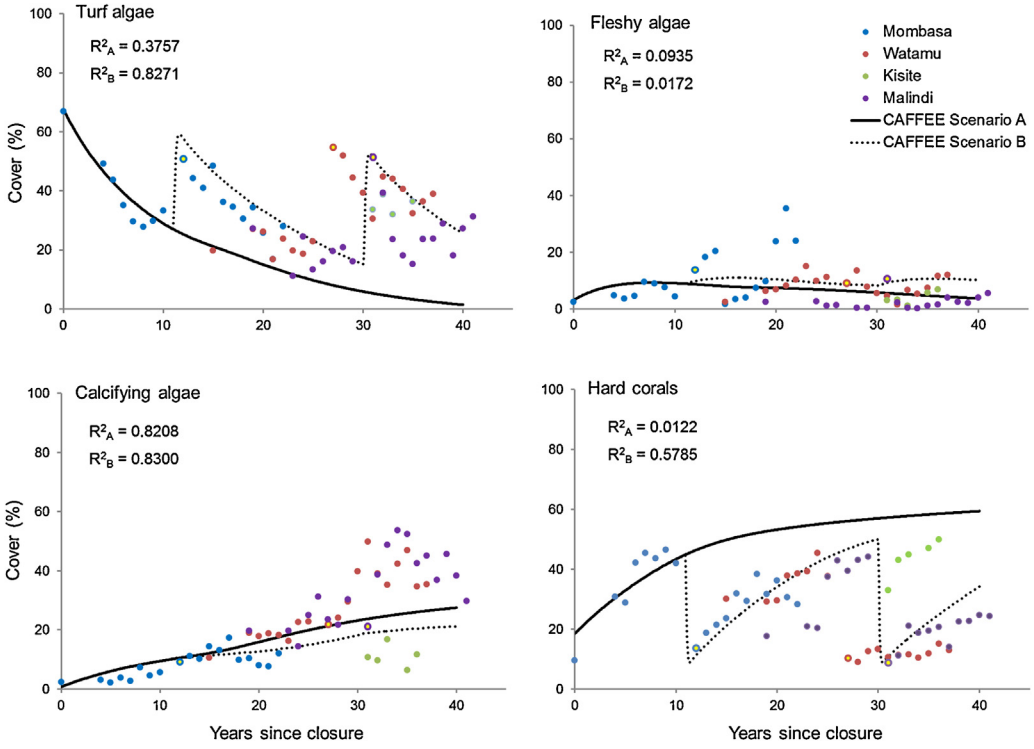

Fig. 5. Benthic cover in Kenyan reefs. Comparison of benthic cover percentage between a long-term observational data set from field surveys in protected Kenyan reefs (data points) and simulations for scenario A (solid line) and B (dotted line) generated with the CAFFEE model. Data points with yellow interior correspond to the 1999 observation. Coefficients of determination (R^2) between the observational data set and model simulations for scenarios A and B are given for each functional group.

where PK_i is the mass of calcium carbonate deposited (Eq. (25)), SA_i is the surface area (Eq. (29)), kd_i is the mass density of coral skeleton, la_i is the fraction of the volume of deposited carbonate resulting in lateral expansion, and *cor* is a coral–coral overgrowth reduction factor. Mass density of coral skeleton was estimated as 1.5 g cm^{-3} and 1.91 g cm^{-3} for massive and branching forms respectively based on the average of values in Carricart-Ganivet et al. (2008), Hughes (1987) and Mallela (2007). The lateralization factor (la_i) is highly dependent on colony radius and branching complexity and we have estimated values of 0.0055 and 0.0078 for massive and branching forms respectively. Coral-coral overgrowth reduction has been parameterized as a sigmoid function of total coral cover, as:

$$cor = \frac{1}{1 + 10^{4\cdot(S_{MC}+S_{BC})-2}} \tag{34}$$

Total lateral expansion has been apportioned proportionally to the relative cover of overgrown substratum type, as:

$$SE_{ij} = SE_j \cdot \frac{S_i}{S_T + S_{TA} + S_{FA} + S_{CA}} \tag{35}$$

2.7. Fisheries

Coral reef fisheries are dominated by artisanal techniques using a variety of gears, including traps, beach seine nets, gill nets, hand lines and spear guns (Jiddawi and Öhman, 2002; McClanahan et al., 2008; van der Elst et al., 2005). Gear characteristics and fisheries methods result in selective catches where certain functional groups are caught more frequently than others (Cinner et al., 2009).

Equation (2) defined F_i as the biomass of fish group *i* captured by fisheries. This term can thus be formulated as $F_i = \Sigma_j F_{ij}$ where F_{ij} is the amount of fish *i* captured by fishery *j*. The total fishery catch for fishery *j* (denoted as FC_j) can be formulated as $FC_j = \Sigma_i F_{ij}$. The partial catch F_{ij} can be parameterized as a function of fishing effort, gear-guild selectivity and fish biomass and catchability, as in the equation:

$$\frac{dF_{ij}}{dt} = nf_j \cdot mt_j \cdot \Sigma_j \psi_{ij} \cdot \frac{B_i}{B_i^0}, \tag{36}$$

where nf_j represents fishing effort as number of fishermen per hectare, mt_j is the maximum daily take per fisherman, ψ_{ij} is the catch ratio of guild *i* by fishery *j*, B_i is the biomass of guild *i* and B_i^0 is a pre-fisheries reference biomass of guild *i*. Catch composition data on artisanal fisheries were used to calculate the fisheries catch-guild ratios (ψ).

The present paper focuses on recovery of reefs from fishing and coral mortality and fishing effort is set to zero. Subsequent studies will examine the influences of fishing on the reef ecosystem.

2.8. Bleaching events

A coral bleaching event is the loss of the coral's photosynthetic symbionts resulting in a reduction in autotrophic production. As a consequence of this reduction, coral metabolic demands and ecological interactions result in a loss of coral biomass, mortality and reduction of benthic cover. An increase in consumption and heterotrophic production has been postulated as a mechanism to compensate for these losses (Grottoli et al., 2006). These processes have been taken into consideration in CAFFEE by including two factors in the energy budget of corals (Eq. (6)): sr_i, which is a symbiont ratio in coral group *i*; and hc_i, which is a heterotrophic compensation factor for coral group *i*. The coral energy budget including bleaching events is then expressed as:

$$\frac{dB_i}{dt} = [B_i \cdot (sr_i \cdot gp_i - r_i - ep_i - ed_i - ac_i) + ae_i \cdot pe_i \cdot \Sigma_j B_i \cdot hc_i \cdot c_{ji}] \cdot (1 - ca_i) - \Sigma_k B_k \cdot c_{ik} \tag{37}$$

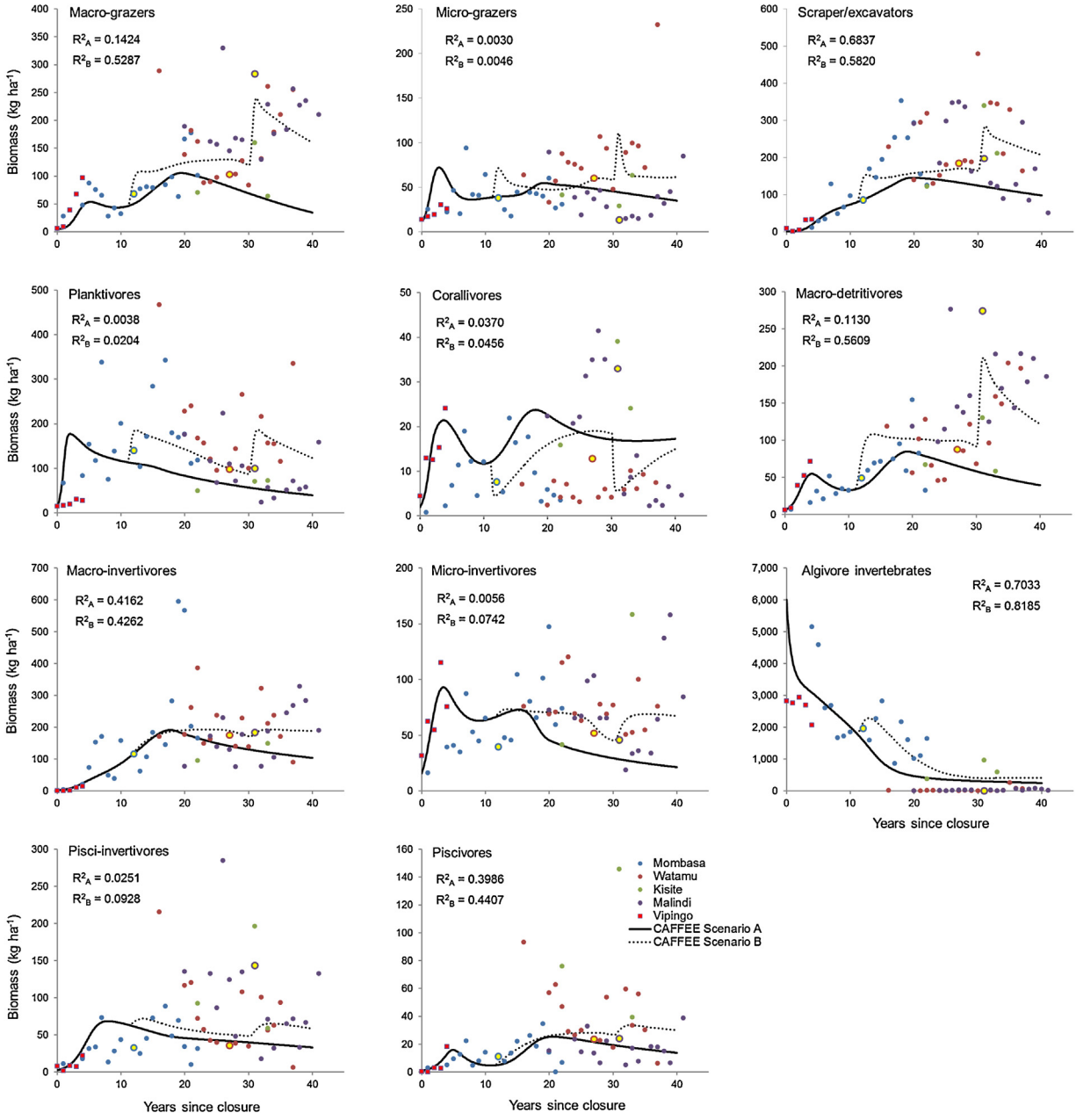

Fig. 6. Fish and invertebrate biomass in Kenyan reefs. Comparison of fish and invertebrate biomass between a long-term observational data set from field surveys in protected Kenyan reefs (data points) and simulations for scenario A (solid line) and B (dotted line) generated with the CAFFEE model. Data points with yellow interior correspond to the 1999 observation. Coefficients of determination (R^2) between the observational data set and model simulations for scenarios A and B are given for each functional group.

The symbiont ratio is a relative measure of symbiont biomass defined as the ratio between current and average values. As symbiont dynamics are not explicitly modeled in CAFFEE, this ratio is assumed to be 1 except while recovering from the effects of a simulated bleaching event. We have assumed that symbionts are re-acquired by corals at a constant rate and have parameterized symbiont ratio as:

$$sr_i(t) = 1 - \mathrm{BE}_{\mathrm{int}} + \mathrm{BE}_{\mathrm{int}} \cdot \mathrm{BE}_{\mathrm{rr}} \cdot (t - t_{\mathrm{BE}}) \quad (38)$$

where $\mathrm{BE}_{\mathrm{int}}$ is the intensity of the bleaching event, given as the fraction of symbionts lost, $\mathrm{BE}_{\mathrm{rr}}$ is the coral's rate of recovery of symbionts, and t_{BE} is the time of the bleaching event. These three parameters are mandatory inputs for simulations including bleaching events.

2.9. Model calibration

Conceptually, the CAFFEE food web and its associated processes are representative of East African coral reefs, but given that regional ecophysiological studies are scarce, most parameters used in calibrating CAFFEE have been extracted from studies realized elsewhere. These values have been either used directly as presented in their original publications or derived using standard conventions or related literature. These conversions are listed in Table s.9 in the supplementary material. Values for parameters such as preyability indices, competition coefficients and non-predatory mortality rates have been indirectly derived from heuristic model runs of the computer model.

CAFFEE has been implemented as a computer application using STELLA Modeling and Simulation Software (version 9.1.4). Model

Table 2
State variables and productivity ratios for benthic functional groups in scenario A and B simulations. B_0 and B are initial and final biomass density (in kg ha^{-1}); S_0 and S are initial and final benthic space occupied (as a fraction of total); and K_0 and K are initial and final skeleton mass (in kg $CaCO_3$ ha^{-1}). P_n:B is an estimate of the annual net production to biomass ratio (calculated as factor of the instantaneous ratio, not accumulative). P_g:R is the instantaneous gross productivity to respiration ratio. NPP is an estimate of the aerial daily net productivity. Values for these ratios are shown as average ± standard deviation of the values obtained at 30-day intervals throughout the 40-year simulation run.

Functional group	B_0	B	S_0	S	K_0	K	P_n:B	P_g:R	NPP (g C m^{-2} d^{-1})
Scenario A									
Turf algae	7509.67	246.07	0.6745	0.0139	–	–	20.09 ± 0.97	1.84 ± 0.04	0.626 ± 0.531
Fleshy algae	1527.34	1897.51	0.0313	0.0366	–	–	8.85 ± 0.99	2.93 ± 0.23	0.239 ± 0.054
Calcifying algae	22.80	1278.57	0.0076	0.2749	2000	174,729.01	10.47 ± 1.25	2.26 ± 0.17	0.122 ± 0.060
Seagrass	469.70	1155.62	0.0154	0.0299	–	–	4.32 ± 0.59	1.57 ± 0.08	0.056 ± 0.008
Massive corals	866.97	5661.70	0.0889	0.2683	30,000	994,959.31	1.65 ± 0.24	1.16 ± 0.02	0.195 ± 0.040
Branching corals	748.80	4306.34	0.0960	0.3256	42,000	1,518,241.20	2.53 ± 0.29	1.15 ± 0.02	0.230 ± 0.045
Scenario B									
Turf algae	7509.67	4431.03	0.6745	0.2565	–	–	20.97 ± 0.97	1.88 ± 0.04	1.175 ± 0.379
Fleshy algae	1527.34	4365.39	0.0313	0.1014	–	–	9.79 ± 0.72	3.15 ± 0.16	0.323 ± 0.047
Calcifying algae	22.80	890.71	0.0076	0.2116	2000	123,360.41	11.32 ± 0.89	2.37 ± 0.12	0.101 ± 0.043
Seagrass	469.70	827.51	0.0154	0.0242	–	–	4.87 ± 0.44	1.64 ± 0.06	0.053 ± 0.005
Massive corals	866.97	3663.06	0.0889	0.1715	30,000	282,557.40	1.72 ± 0.82	1.17 ± 0.08	0.134 ± 0.075
Branching corals	748.80	2213.36	0.0960	0.1705	42,000	203,252.54	2.66 ± 1.41	1.15 ± 0.08	0.135 ± 0.087

simulation runs presented in this paper used a time-step of 0.25 days which smoothed the integration of microbial and higher-level functional groups.

2.10. Model validation

To validate our model, we used a data set of fish and invertebrate biomass and benthic cover observations compiled over the past 20 years, with the first observations dating back to 1988. This data set includes observations recorded in 8 study areas along the Kenyan coast and includes coral reefs that have been afforded protection or fisheries closure status at different times during the time frame of this data set (Table s.10 in the supplementary material). It also includes sites that have been exempt from protection and that have been extensively used as fisheries grounds. We extracted subsets from this data set to compare reef dynamics between observed data and simulations from the model. In particular, we compared the dynamics of state variables such as biomass of fish and invertebrate functional groups or percentage cover of benthic space with field data. The following scenarios were examined:

Scenario A – Reefs closed to fishing (protected): We used observational data from 4 study areas that have been closed to fishing for a time interval ranging from 43 years (Malindi) to 6 years (Vipingo) and constructed a 40-year time-overlap series of reef recovery from fishing. Initial values of functional group biomass and benthic cover were obtained from the first observations in the data set and used as initial conditions in 40-year model simulations. Reefs at the time of closure had low fish biomass and were generally dominated by sea urchins and associated states of the benthic community (O'Leary and McClanahan, 2010).

Scenario B – Protected reefs and bleaching events: Using the same initial conditions as in the previous scenario, we ran model simulations including a bleaching event designed to resemble the 1998 massive bleaching event that caused severe bleaching and coral mortality in Kenyan reefs (McClanahan et al., 2001). We parameterized this event in our model using a bleaching intensity of 80%, symbiont recovery rate of 0.007 d^{-1} and heterotrophic compensation of 1 (i.e. no increase in heterotrophy). This scenario represents the context for the empirical field data where the dual effects of recovery from fishing and a large temperature anomaly and associated coral mortality influenced the observational time series (McClanahan, 2008).

3. Results and discussion

3.1. Model fit to observational data

The percentage of benthic cover and the biomass of fish and invertebrate functional groups in the CAFFEE simulations for scenarios A and B indicate the importance of using simulations that realistically reflect the observational data (Figs. 5 and 6). The data set of benthic cover observations in Kenyan reefs protected from fishing offers a good reference for the drastic shift in coral reef benthic communities after the 1998 massive coral mortality. The simulations generated by the CAFFEE model for scenario A (without bleaching events) showed staggered changes reflected in declining turf algae over the full time series, a small rise and subsequent decline in fleshy algae a few years after the closures and a 20 year recovery of hard coral from 20% to 60% cover, and slow continuous rise in calcifying algae for the full 40 years (Fig. 5). This pattern may be realistic for changes associated with reef recovery from fishing and high sea urchin abundance and grazing (O'Leary and McClanahan, 2010) but showed poorer fits with the observed values of reef cover for hard corals and turf algae that were disturbed by the 1998 thermal anomaly (Fig. 5).

When the 1998 bleaching event was included in the simulations (scenario B), the fit with observational data improved considerably for hard corals and turf algae. Kenya's protected reefs comprised as much as 40% coral cover before the bleaching event but cover was reduced to ~10% after the event (Fig. 5; McClanahan et al., 2001). In the simulation, the main beneficiary of this coral mortality was algal turf, which increased from ~30% to almost 60% of the total cover. The cover of fleshy algae increased slightly and calcifying algae decreased slightly after bleaching in the simulation. Field data from Kenyan sites after the 1998 bleaching showed an increase in turf algae from 31 to 59%, fleshy algae increased from 5% to 10% of the cover, and the two groups of calcifying algae (red and green) showed different responses but an overall decline of 32% of their initial cover (McClanahan et al., 2001). The model responses are similar to the field data but there is some evidence that red calcifying algae underwent a recovery a few years after the bleaching event (O'Leary and McClanahan, 2010), which was not evident in the simulation where the fleshy algae stayed above and the calcifying algae stayed below the control run over time. It should be noted that, because the studied reefs were at different ages of protection when the bleaching event occurred, our simulations included the simulated bleaching event at two different times, producing a saw-shaped simulation that corresponds to the observational data

in the year and time since closure to fishing that the bleaching occurred.

Initial and final biomass, benthic cover and skeletal mass for the simulations in scenario A led to coral-dominated benthic communities, where hard corals occupied 60% of benthic space, calcifying algae 27.5%, and the rest of the macrophyte groups combined made up 8% (Table 2). Scenario B simulations by contrast resulted in a turf and fleshy algae cover of almost 40% while hard coral was only 34% of benthic space. Consequently, thermal disturbances may explain some of the unexpected changes seen in these protected reefs over the period of closure from fishing (McClanahan, in review).

The two scenarios also influence the fish and sea urchins changes in the simulations and probably in the observational data (Fig. 6; McClanahan et al., 2002a). Scenario A simulations showed general increases in most fish groups over time and a steady decline in sea urchins over the first 20 years of closure. There are also small declines in fish biomass in the final years of the simulation that are associated with changes in benthic cover and associated productivity but also changes in food sources and trophic interactions of the different functional groups. For example, herbivore biomass declined with the reduction of macrophyte cover and aerial productivity of turf algae (Fig. s.5c), leading to an increased intake of dietary items with less productivity (Fig. s.7). A previous empirical evaluation of these fisheries closures reported a decline in biomass and suggested it was associated with increased calcifying algae and reduced net production in the oldest closures (McClanahan and Graham, 2005), which is seen in the model's benthic productivity trajectories (Fig. s.5).

The model trajectories for the biomass of fish and invertebrate groups were clearly different between scenario A and B simulations for the primary consumers functional groups but similar for the higher trophic levels. Scenario B trajectories generally had a much better fit to the field data than those of scenario A indicating bleaching effects on the consumer groups with coral mortality (Wilson et al., 2006). For all the fish and invertebrate groups, except for corallivores, biomass levels at the end of the simulation were elevated in the bleaching scenario relative to the recovery from fishing without bleaching (Table 3). Large grazers and detritivores in particular had strong responses to the reversal to turf-dominated benthos derived from bleaching events. Fish biomass in these groups at the end of the simulation with bleaching was two- to four-fold that of the non-bleaching scenario. In contrast, corallivore biomass declined sharply following bleaching events but recovered steadily afterwards reaching similar levels at the end of the simulations in both scenarios. Observational data after bleaching events has shown increases in surgeonfish, mostly detritivorous types such as *Ctenochaetus*, but also some browsers and declines in coral-eating butterflyfish (Chong-Seng et al., 2012; McClanahan et al., 2002a). Sustained increases in herbivore biomass associated with high levels of turf and coralline algae after severe bleaching have also been reported in western Australian reefs (Gilmour et al., 2013). Carnivorous fish groups had weakly positive immediate responses to bleaching events but maintained elevated biomass at the end of the bleaching scenario, in contrast with the steady biomass decline in the scenario without bleaching. Some fish that feed on micro-invertebrates, such as angelfish and mixed feeders, can also increase along with piscivores but responses can overall be mixed, weak, species specific, and time and disturbance-intensity dependent (Chong-Seng et al., 2012; Pratchett et al., 2008). The model, therefore, predicts fish are most influenced by organic production increases and trophic interaction that occur when algae and its productivity increases and possibly less reliable concerning habitat requirements, which can often be reflected in the losses of sensitive fish species after coral mortality (Chong-Seng et al., 2012; Graham et al., 2008, 2011).

Table 3
Biomass and ratios of pelagic functional groups for the simulations in scenarios A and B. B_0 and B are initial and final biomass density (kg ha^{-1}). Production turnover (P_n:B) and consumption rate (C:B) are annual rates (factored from the instantaneous rates, not accumulative) and are shown as the average and standard deviation of values obtained at 30-day intervals throughout the 40-year simulation runs. The values of P_n:B and C:B in the Literature column are given for comparison purposes and were extracted from the works of Bozec et al. (2004) and Opitz (1996).

Functional group	Scenario A				Scenario B			Literature	
	B_0	B	P_n:B	C:B	B	P_n:B	C:B	P_n:B	C:B
Microplankton	30	26.75	361.07 (102.07)	164.25 (0.00)	24.75	445.32 (75.50)	164.25 (0.00)	70[a]	–
								511[a]	–
Zooplankton	120	25.83	18.28 (3.06)	152.54 (18.95)	99.18	16.36 (2.55)	140.70 (15.74)	40	165
								416	1178
Micro-invertebrates	800	150.92	4.32 (1.20)	36.74 (4.67)	603.88	3.66 (0.84)	34.95 (3.78)	1.8–4.14	20–125.5
Detritivore invertebrates	150	41.03	1.40 (0.25)	8.00 (1.26)	113.80	1.46 (0.29)	8.35 (1.47)	0.29–2.23	3.36–14.4
								0.86–2.3	5.6–7.5
Corallivore invertebrates	5	37.88	1.63 (0.56)	12.28 (2.55)	22.38	1.53 (0.68)	11.82 (3.12)	0.49–2.5	3.24–14
								3	7.92
Algivore invertebrates	6000	248.53	0.88 (0.40)	8.23 (2.26)	410.92	0.86 (0.39)	8.10 (2.19)	0.34–2.5	3.7–14
								2.3	9.42
Macro-grazer fish	6.05	34.47	0.59 (0.14)	22.72 (1.24)	160.66	0.64 (0.20)	23.16 (1.80)	0.6–0.71	23.6–25.65
								0.68	20.42
Micro-grazer fish	12.68	34.95	1.14 (0.14)	30.49 (1.24)	61.61	1.21 (0.25)	31.13 (2.24)	0.68–2.84	12.4–36.1
								1.91	29.63
Scraper-excavator fish	1.2	97.86	0.63 (0.18)	27.21 (1.49)	207.43	0.69 (0.21)	27.69 (1.73)	0.85–1.15	13.5–33.9
Planktivore fish	14.43	39.89	1.25 (0.32)	19.73 (2.04)	123.27	1.64 (0.27)	22.22 (1.70)	0.68–3.54	12.4–43.4
								0.93–1.35	8.8–10.72
Macro-detritivore fish	6	39.49	0.71 (0.10)	18.35 (0.69)	122.03	0.78 (0.22)	18.81 (1.57)	–	–
Micro-detritivore fish	10	18.33	1.20 (0.22)	27.38 (1.50)	64.28	1.43 (0.37)	28.91 (2.49)	1.5–3.14	16–39.7
								1.33	16.3
Corallivore fish	2	17.27	1.52 (0.13)	27.12 (0.87)	14.97	1.45 (0.39)	26.61 (2.59)	–	–
Macro-invertivore fish	2	103.68	0.73 (0.06)	9.54 (0.31)	188.65	0.79 (0.01)	9.83 (0.06)	–	–
Micro-invertivore fish	16	21.30	1.09 (0.22)	12.33 (1.34)	67.06	1.30 (0.08)	13.66 (0.50)	1.6–3.82	9.8–14.65
								1.15	9.96
Pisci-invertivore fish	2.5	33.18	0.45 (0.15)	6.73 (0.86)	58.47	0.56 (0.10)	7.36 (0.57)	0.47	5.24
Piscivore fish	1	13.82	0.34 (0.22)	6.69 (1.15)	30.02	0.46 (0.24)	7.33 (1.22)	0.24–1.26	2.3–12.5
								0.39–0.48	3.99–4.71

[a] Phytoplankton only.

3.2. Ecosystem productivity

Annual net productivity to biomass ratio (P_n:B) of benthic macrophytes (Table 2) showed average production turnover rates in the Scenario A simulations ranging from 4.32 yr^{-1} for seagrasses to 20.09 yr^{-1} for turf algae. All benthic groups experienced slight (4–12%) productivity increases in the Scenario B simulations. These ratios remained fairly constant during the 40-yr simulations (Fig. s.5a) with only the turf algae showing a moderate and pulsed increase in productivity response after bleaching events. The P_n:B ratios obtained were similar to production turnover values used in Ecopath models by Bozec et al. (2004), Opitz (1996) and Tudman (2001), and similar temporary increases in net production have been reported in bleached reefs (Kayanne et al., 2005). The annual production turnover of hard corals in the simulations was 1.72 yr^{-1} and 2.66 yr^{-1} for massive and branching forms respectively (in Scenario B); these values are slightly higher than the values (0.37–1.8 yr^{-1}) used in Opitz (1996). These ratios were fairly constant throughout the simulation except for the period following the simulated bleaching events where P_n:B reached temporary minima below −7 and −12 for massive and branching corals respectively (Fig. s.5a).

Productivity-respiration ratios P_g:R in turf algae (1.88 ± 0.04) were fairly constant throughout the simulation, with values that are lower than what has been described in the literature. For example, turf algae P_g:R ratios of ∼3 have been reported by Dhargalkar and Shaikh (2000) and by Rogers and Salesky (1981) whereas Carpenter (1985) estimated a range of P_g:R values for turfs of 4.19–7.29. Fleshy algae P_g:R ratio showed little variation (Fig. s.5b) around the average value of 3.15, a value well in the range of those reported in other studies (Dhargalkar and Shaikh, 2000; Rogers and Salesky, 1981; Wanders, 1976a,b). On the calcifying algae, the P_g:R ratio was also fairly constant throughout the simulation, with a value of 2.37 ± 0.12, similar to those reported by Chisholm (2003), Martin et al. (2006) and Wanders (1976a). With respect to seagrasses, their P_g:R ratio was also constant throughout the simulation, and its average value of 1.64 ± 0.06 was slightly higher than previous found in a field study by Ziegler and Benner (1999).

Overall daily benthic production in the scenario A simulation was 1.47 ± 0.41 g C m^{-2} d^{-1}, with 42.6%, 28.9% and 16.2% corresponding to turf algae, hard corals, and fleshy algae, respectively (Table 2). A comparatively higher benthic production of 1.92 ± 0.30 g C m^{-2} d^{-1} was found with the scenario B simulations, with the main contributors being turf algae (61.2%), fleshy algae (16.8%) and hard corals (14.0%). These scenarios reflect the trade off in inorganic (calcium carbonate) and organic production in coral reefs that can be influenced by bleaching and coral mortality (McClanahan et al., 2002b).

The P_n:B ratios of consumer functional groups where generally in good agreement with comparable values in other coral reef ecosystem models (Table 3) although some fish groups (scraper-excavators, micro-detritivores and micro-invertivores) had comparatively lower production turnover values. Most groups had higher P_n:B ratios in Scenario B simulations as they benefitted directly or indirectly from increased benthic organic production. One obvious exception was the corallivorous groups where P_n:B and biomass decreased as a consequence of the reduction in consumption. Zooplankton and micro-invertebrates also had slightly lower P_n:B ratios in the bleaching scenario but their standing stocks increased, suggesting a reduction in predation intensity by corals for the former, and by macro-invertivores for the latter.

3.3. Consumption processes

The biomass-specific consumption rates of the consumer functional groups values are, in general, in agreement with C:B ratios used in other coral reef trophic models (Table 3). Overall, there were only minor differences in C:B ratios between the two scenarios, with Scenario B elevating consumption and production in the fish consumers relative to Scenario A, due to greater organic than inorganic production in Scenario B. The most common effect of the thermal anomaly on consumption rates was a short-term increase in herbivorous and detritivorous group consumption and decrease in corallivores (Fig. s.6). This increase in consumption and temporary increases in the biomass of herbivore/detritivores have been observed after mass mortalities of sea urchins and bleaching events (McClanahan et al., 2002a; Robertson, 1991). More complex responses of consumption rates to the thermal anomaly were observed in planktivores, piscivores, pisci-invertivores and micro-invertivores where bleaching resulted in a longer-term elevation of consumption rates, which can be associated with the increased availability of food sources with higher productivity levels. Thus, the increase in planktivore fish feeding rates follows from high POM production rates, mostly by macrophytes, after bleaching events (see Section 3.5), and piscivores and pisci-invertivores increased their dietary intake of food items with higher productivity (e.g. planktivores, micro-detritivores) (Fig. 7). Piscivores are generally least affected by coral mortality, and it might be expected that their prey are easier to capture after coral mortality although this is not a well-studied aspect of reef ecology studies (Wilson et al., 2006). Nevertheless, Pistorius and Taylor (2009) have suggested that there is a delayed effect of coral mortality on piscivorous fish based on a time series of catches in the remote Aldabra reefs.

The trajectories of the diet composition of the consumer functional groups in Scenario A indicate a transition from an algae–herbivores-dominated ecosystem to a coral–carnivores-dominated ecosystem as the time since stopping fishing increased (Fig. 7; Fig. s.7 in the supplementary material). Herbivorous fish shifted their diets toward an increase in their intake of seagrass and calcifying algae once algal turf became less abundant, which reflects the many studies that find diet changes from poorly to highly defended plants with increased herbivory (Hay, 1996). Additionally, the transition from organic production with low trophic dominance to inorganic production and higher trophic levels is commonly reported and a dominant paradigm in reef ecology (DeMartini et al., 2008; McClanahan and Shafir, 1990; Sandin et al., 2008). The bleaching events in Scenario B simulations strongly modified the overall organic to inorganic production and herbivores maintained a more regular diet composition due to the resetting effect of bleaching mortality on benthic cover toward early successional algae.

The diet of macro-invertivores, mainly urchins at the beginning of the simulations, became mostly micro-invertebrates after 17 years for Scenario A and after 23 years in Scenario B (Fig. s.7 in the supplementary material). Bleaching increases the persistence of the algivore and detritivore invertebrates and reduced corallivore and micro-invertebrates in the diet of macro-invertivores. Corallivores increased the consumption of massive over branching corals and planktivores increased the zooplankton diet fraction over pelagic POM for a few years after the bleaching event. Corallivores are the best studied group (Cole et al., 2008), and switching diets is commonly observed for corallivores from studies of the same species in locations with different prey but consumption of massive species has also been shown to reduce the health of some butterflyfish (Berumen et al., 2005; Berumen and Pratchett, 2008; Graham, 2007). Nevertheless, there are many non-butterflyfish that feed on massive species and some were observed to do considerable damage to massive *Porites* after the 1998 bleaching event (McClanahan et al., 2005).

Changes in feeding of the same species across bleaching events have not been studied but the response is expected to be species-dependent, influenced by the fidelity of their diet and obligate coral

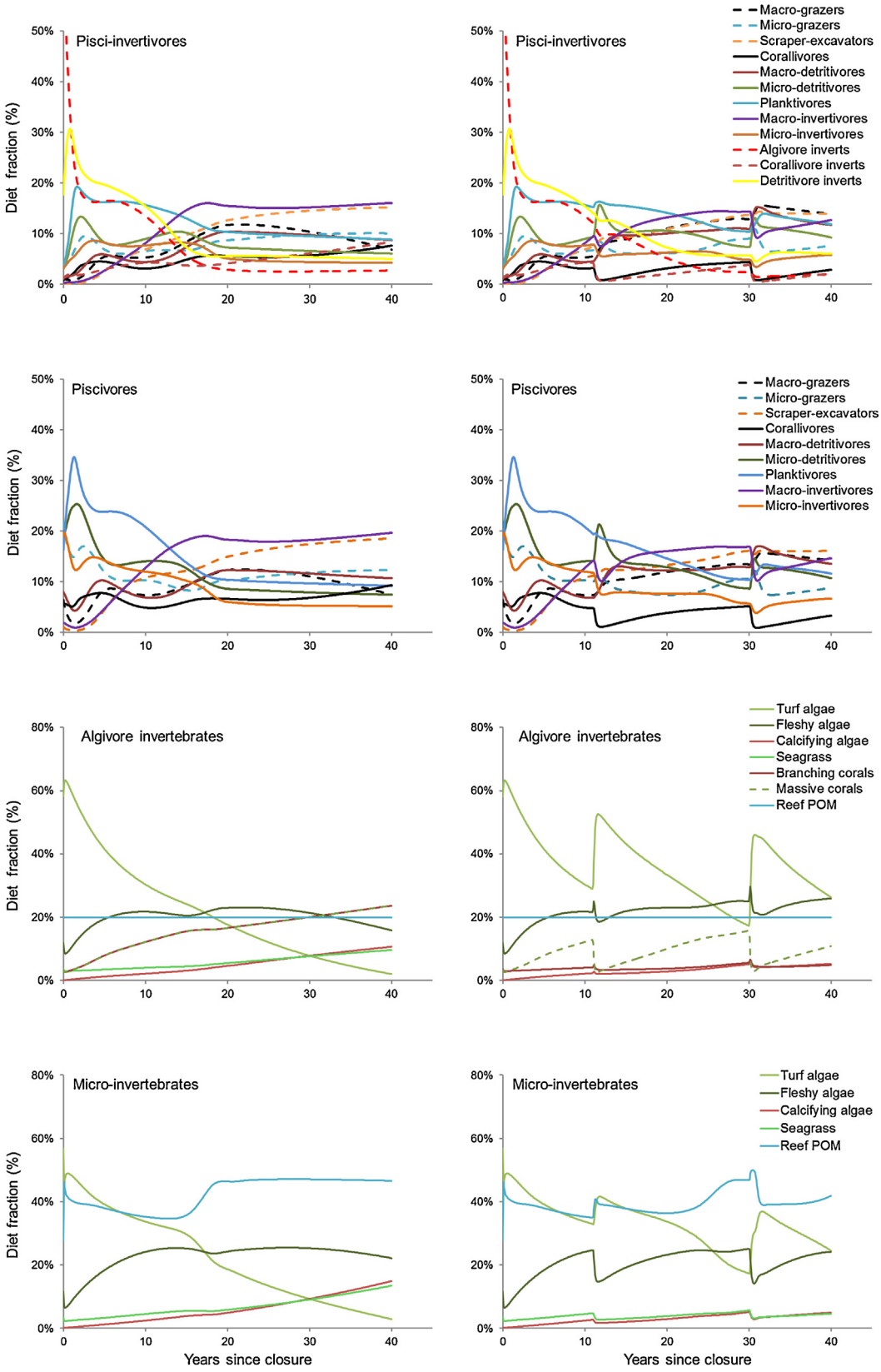

Fig. 7. Diet fractions. Trajectories of the dietary composition of selected functional groups during the CAFFEE simulations for scenario A (left column graphs) and scenario B (right column graphs). Graphs for the rest of the functional groups can be seen in Fig. s7 in the supplemental materials.

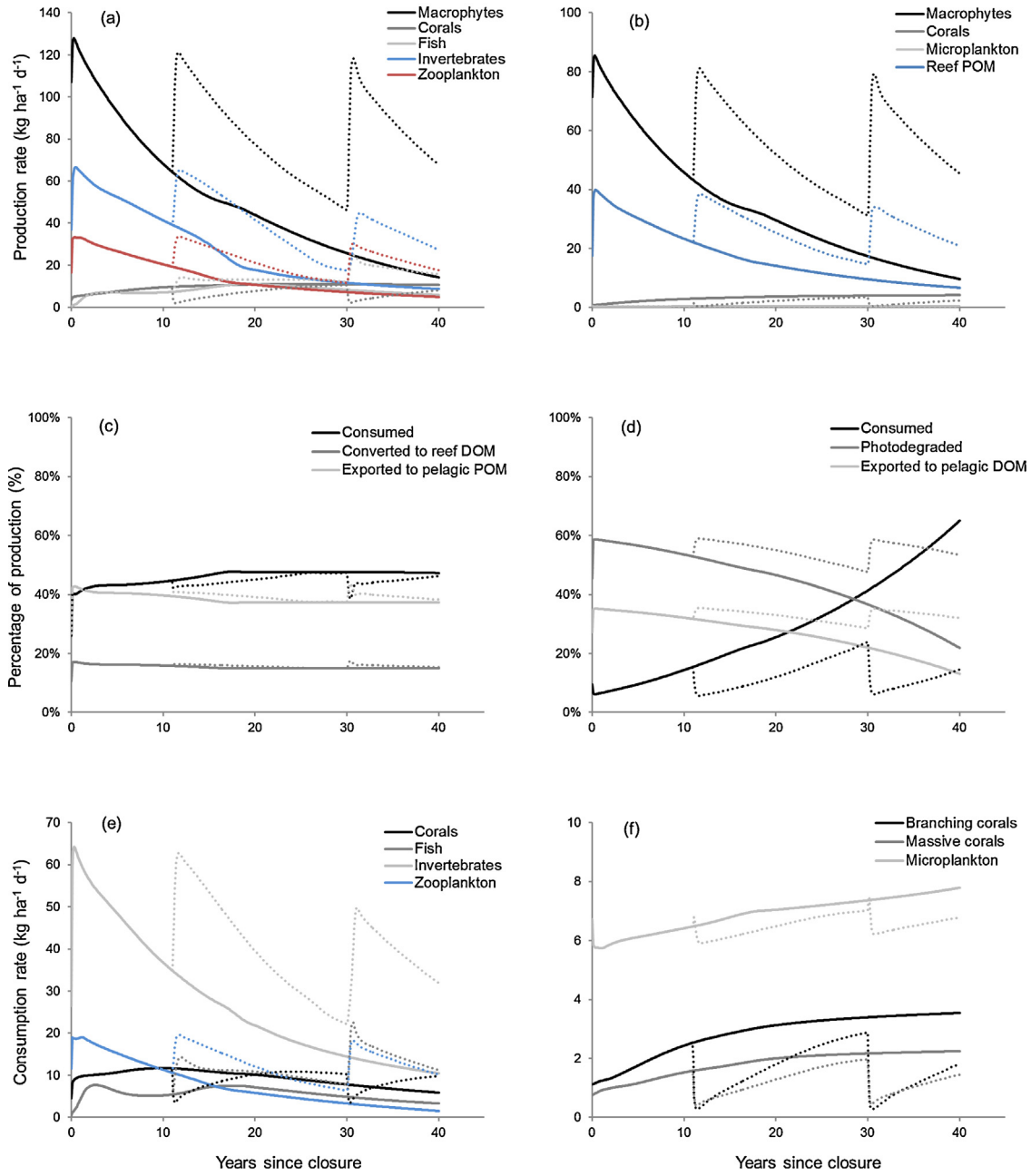

Fig. 8. Energy dynamics of reef detritus. CAFFEE simulations for scenario A (solid lines) and scenario B (dotted lines). (a) Production rate and sources of reef POM and (b) DOM, (c) utilization of reef POM and (d) DOM production, (e) consumption rate of reef POM and (f) DOM.

feeder populations often decline while facultative coral feeders show little change after high levels of coral mortality (Pratchett et al., 2006). Fewer studies have been undertaken on diet changes in macro-invertivores after reduced fishing effort and bleaching but this gross pattern of switching to smaller invertebrates is consistent with other types of disturbances, such as declines in sea urchins (Robertson, 1987).

3.4. Energy balance

Stopping fishing in the model resulted in an initial increase in biomass growth rate for all consumer functional groups except for the algivore invertebrates (Fig. s.8 in the supplementary material), followed by a steady decline which stabilized at growth rates between ±0.02% biomass per day about ten years into the simulations. Scenario B simulations showed peaks of positive growth rate around bleaching events in all groups except for corallivores. Empirical studies of the early stages of fisheries closures frequently report rapid recovery among fast-growing species but a decline in growth and slow recovery in the later stages after closure (McClanahan et al., 2008; Russ and Alcala, 2004).

The trajectories of the ratios of respiration, predation and non-predatory mortality to the biomass produced throughout the simulations indicated that metabolic respiration used 30–70% of the produced energy in most groups, with predation generally taking a secondary role of 20–30% of the production (Fig. s.9). Non-predatory mortality showed peaks of production utilization in contexts of reduced predation.

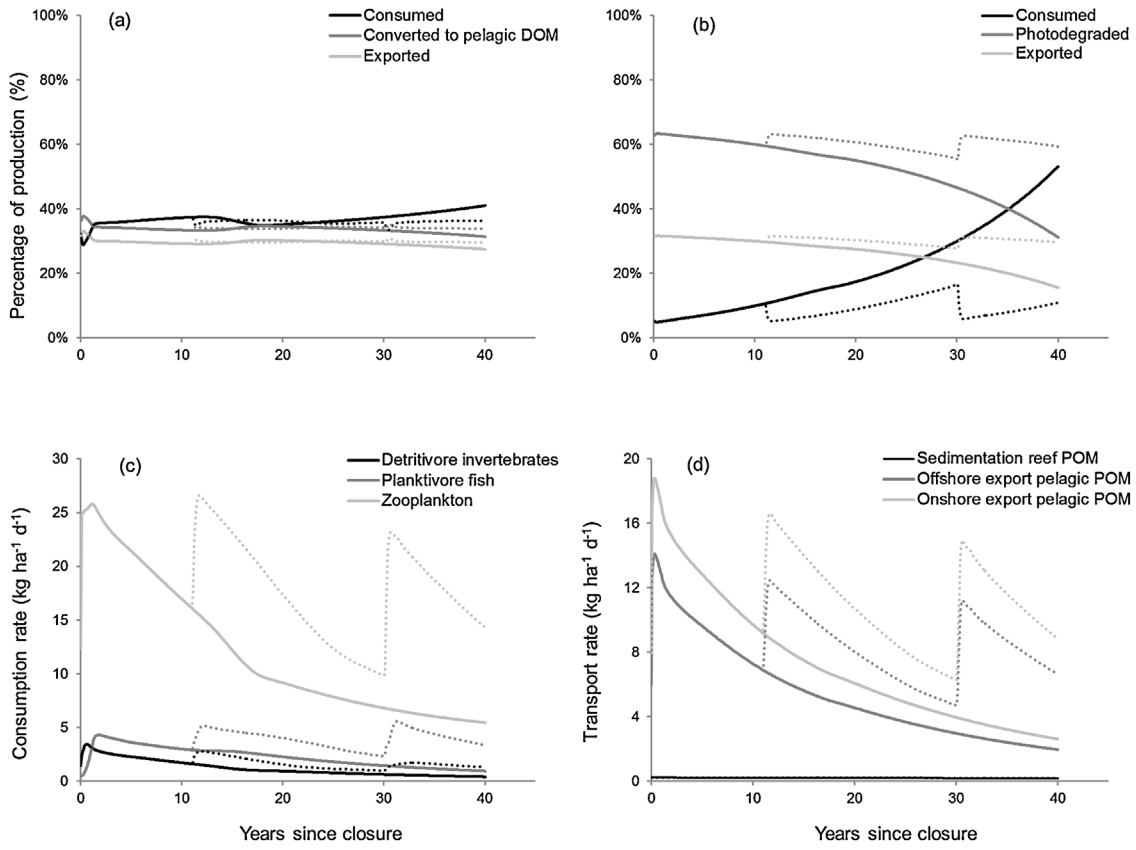

Fig. 9. Energy dynamics of pelagic detritus. CAFFEE simulations for scenario A (solid lines) and scenario B (dotted lines). (a) Utilization of pelagic POM and (b) DOM production, (c) consumption rate of reef POM and (d) export rates of reef and pelagic POM.

3.5. Flow of detrital organic matter

Algae fragments, followed by invertebrate and zooplankton excreta and carcasses, dominated the production of POM in all the simulations (Fig. 8a). Lesser contributions to the POM pool were from the organic releases of fish and corals. In the Scenario A, POM production from all sources decreased as the time since fishery closure increased, which was driven by the reduction in benthic macrophyte cover, so that fish and coral POM release play a larger relative role by the end of the 40 year simulation. Bleaching events in Scenario B had the effect of re-setting the reef POM production to higher levels as algae dominated the reef again. Reef DOM dynamics followed the same patterns (Fig. 8b), with a substantial contribution from reef POM into DOM production.

The model's patterns of organic release are consistent with experimental observations where algae are reported to release greater organic carbon than corals (Haas et al., 2011). This creates increased microbial populations and oxygen demand that have been observed across fishing and nutrient gradients (Haas et al., 2009, 2011). A gradient of exposure to different levels of fishing in the Pacific found patterns in line with our simulations of recovery of fishing effects over time in terms of the benthic cover changes where dominance of inorganic carbon producers increased and the release of organic carbon was reduced with declining fishing impacts (Sandin et al., 2008; Haas et al., 2011). Field studies also indicate that bleaching and coral mortality rapidly increases algal cover and the release of DOC and POC, which stimulates microbes, of which some may promote diseases that are frequently reported along with increases in algae after nutrification, bleaching, and coral mortality (Bourne et al., 2008; Haapkylä et al., 2011; McClanahan et al., 2004; Nugues et al., 2004).

Reef POM produced in the model was either consumed in situ or exported to the water column in similar percentages (~40%) while the remainder (<20%) was converted to dissolved organic matter (Fig. 8c). These values changed little in Scenario B simulations with short-term reductions to consumption due to coral mortality. The proportion of consumed DOM increased in the absence of bleaching events as reef DOM stocks declined and bleaching events had a balancing effect on DOM utilization rates (Fig. 8d). Invertebrates dominated detritus consumption but their role declined over the time since closure to fishing. In contrast, fish, corals and zooplankton had lower and more stable consumption rates of detritus throughout the Scenario B simulations (Fig. 8e), a consequence of high sea urchin and other invertebrate abundance in fished reefs. Bleaching increased the consumption of POM by zooplankton and fish but the loss of living coral tissue led to a decline in their consumption rates of both POM and DOM (Fig. 8f). There was a very temporary increase in the consumption of DOM by microplankton after bleaching but this eventually lead to a lower levels as other groups consumed more POM and DOM. Consumption trends followed POM production rates in their response to reduced fishing and bleaching events, an indication of bottom-up control along this trophic pathway.

Detritus that was exported to the pelagic system in the model had similar dynamics to the detritus maintained in the coral reef (Fig. 9a–c). Detrital matter leaving the system (either buried in sandy sediments, transported offshore or deposited onshore) was approximately 12% of the POM produced in both scenarios ($11.5 \pm 0.6\%$ and $12.0 \pm 0.4\%$, for scenarios A and B respectively; Fig. 9d). Exported POM was mainly in the form of macrophytal detritus deposited on the beach (7.24 ± 3.99 and $11.51 \pm 2.80\ \mathrm{kg\,ha^{-1}\,d^{-1}}$, for scenarios A and B respectively) and transported to pelagic waters surrounding the reef

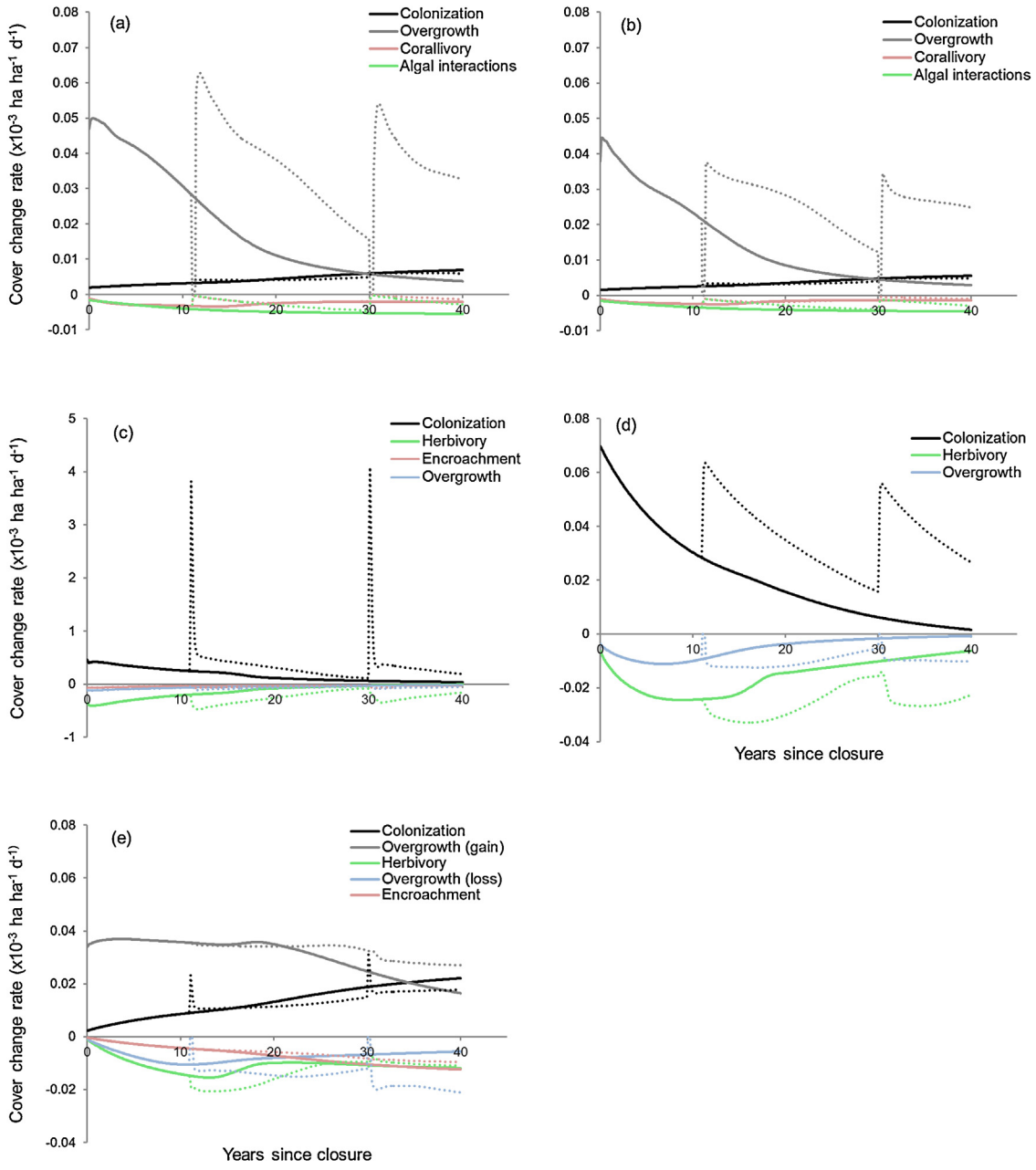

Fig. 10. Dynamics of benthic cover. Reef cover dynamics for (a) branching corals, (b) massive corals, (c) turf algae, (d) fleshy algae and (e) calcifying algae during the CAFFEE simulations for scenario A (solid lines) and scenario B (dotted lines).

($5.43 \pm 2.99\,kg\,ha^{-1}\,d^{-1}$ and $8.63 \pm 2.10\,kg\,ha^{-1}\,d^{-1}$, for A and B respectively). The amount of POM buried in sandy sediments was comparatively much smaller at $0.21 \pm 0.02\,kg\,ha^{-1}\,d^{-1}$ and $0.22 \pm 0.01\,kg\,ha^{-1}\,d^{-1}$ for A and B respectively. The amount of algae and seagrass detritus exported onshore was equivalent to ~2.5% of macrophytal NPP in both scenarios. There are few field studies of the amount of reef algae exported but seagrass studies show highly variable estimates from 1% to 77% of the NPP with average values of around 28% (Heck et al., 2008). Seagrass may be a poor analog for algae, which is expected to be consumed at a higher rate and exported at a lower rate than seagrass.

3.6. Reef space and framework dynamics

Coral lateral expansion, rather than colonization, was the main contributor to coral progressive dominance of benthic cover in the non-bleaching scenario (Fig. 10a and b; Table s.11 in the supplementary material). This trend decreased as coral cover increased and colonization became the main contributor to gaining space 30 years into this simulation as non-calcifying algae cover declined and calcifying algae increased. Field studies have shown that regrowth and lateral expansion is consistently found to be a dominant form of expansion by corals in the early stages of recovery (van Woesik et al., 2011). Coral recruitment rates may be more sensitive to benthic cover conditions and a study in Kenya found higher larval recruitment of corals along a fishing gradient where coralline algae and recruitment rates increased with declining fishing impact (O'Leary et al., 2012).

Corallivory played a relatively small role in cover losses for corals, secondary to mortality by algae, which has been argued to be the most common case for coral reef population dynamics (Mumby, 2009a). Rates of cover loss during bleaching were three orders of magnitude higher than colonization rates and two orders of magnitude higher than algal overgrowth rates (Table s.11 in the

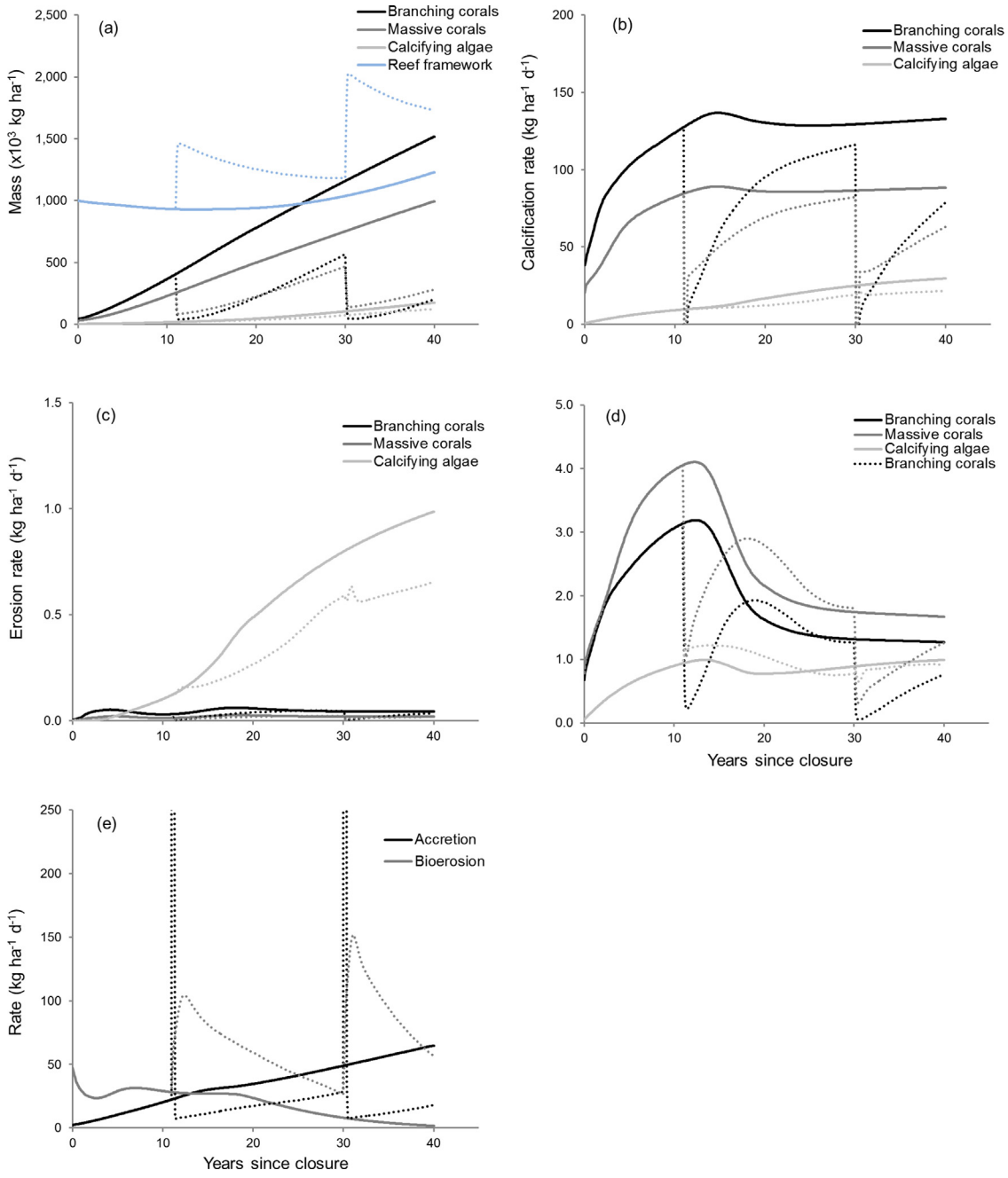

Fig. 11. Reef formation. Trajectories of (a) the standing stocks of reef supporting structures, (b) daily calcification rates of calcifying groups, daily bioerosion rates on calcifying groups by (c) fish and (d) invertebrates, and (e) daily accretion and bioerosion rates on reef framework during the CAFFEE simulations for scenario A (solid lines) and scenario B (dotted lines).

supplementary material). Bleaching, while episodic, is a major contributor to coral loss relative to other sources of mortality, which are more constant but can control responses over longer periods of time (Ledlie et al., 2007; Mumby, 2009b). Herbivory was the main cause of cover loss for all algal groups but the contribution of encroachment and overgrowth in calcifying algae was substantial (Fig. 10c–e). Bleaching events provided short-term boosts to colonization rates for turf algae and, to a lesser extent, to fleshy algae, which is commonly observed on coral reefs after bleaching (McClanahan et al., 2001; Gilmour et al., 2013).

The standing stocks of corals and calcifying algae skeletons increased linearly over time in the Scenario A simulations (Fig. 11a) as a consequence of the positive balance between the rates of reef-forming processes (Table s.12 in the supplementary material). Coral calcification rates stabilized at ~130 kg $CaCO_3$ ha^{-1} d^{-1} and ~85 kg $CaCO_3$ ha^{-1} d^{-1} for branching and massive forms respectively (Fig. 11b) whereas calcifying algae maintained a linear progression in calcification rate reaching 29.2 kg $CaCO_3$ per hectare per day at the end the 40-yr simulation. Field studies produce variable results of about an order of magnitude variation and these values are near averages of reported gross calcification values for growing seaward margins (Davies, 1983; Perry et al., 2012).

Invertebrates were the dominant bioeroding agent in all calcifying groups although fish made a significant contribution to bioerosion of calcifying algae (Fig. 11c and d). Bioerosion rates on coral skeletons by invertebrates peaked at 3.2 kg ha^{-1} d^{-1} and 4.1 kg ha^{-1} d^{-1}, for branching and massive forms respectively, at about 12 years after closure from fishing when sea urchins were

still present and coral cover had recovered to ~40%. Afterwards, once sea urchins declined to low levels, bioerosion on corals stabilized at 1.3 kg ha^{-1} d^{-1} and 1.7 kg ha^{-1} d^{-1} (Fig. 11d). Bioerosion rates on calcifying algae increased steadily along with the recovery of calcifying algae and bioeroding scraping parrotfish, reaching a combined rate of 2.0 kg ha^{-1} d^{-1} at the end of the simulation for scenario A. Empirical studies of reefs recovering from fishing with high sea urchin numbers see direct impacts on corals and the erosion of the calcium carbonate substratum (Carreiro-Silva and McClanahan, 2001; O'Leary and McClanahan, 2010), but unfished reefs largely have high levels of erosion by bioeroding parrotfish, particularly on calcifying algae (Bellwood et al., 2012).

Reef framework declined during the initial 15 years of this simulation as invertebrate bioerosion rates exceeded the rates of reef accretion from the losses of cover of calcifying benthic groups (Fig. 11a and e). Bleaching events had a large effect on reef framework stocks as coral mortality transferred large amounts of coral skeleton to the framework and these pulsed gains far exceeded bioerosion losses (Fig. 11a and e). Daily rates of transfer of coral skeleton mass into reef framework peaked at over 20,000 kg ha^{-1} d^{-1} (Fig. 11e, off-scale), three orders of magnitude greater than the average rates (Table s.12 in the supplementary material). Coral calcification and bioerosion rates showed greater variability in Scenario B simulations (Fig. 11b and d; Table s.12 in the supplementary material) as the change toward greater calcification was restarted after bleaching events.

4. Conclusions

CAFFEE is an integrated energy and materials based simulation model of a coral reef and therefore provides a holistic perspective of these important forcing and productivity aspects of coral reefs. In principle, it provides a control system or possible default model of a coral reef where energy and materials are the main drivers and outputs of the ecosystem, as opposed to more complex species and habitat-specific interactions that are more challenging to understand and model at this large scale. Nevertheless, when comparing the model outputs to functional level empirical field data on benthic cover and fish biomass it provides considerable explanatory value, especially for the more realistic condition of a major bleaching event during the empirical time series. It should also be appreciated that the field data are influenced by other factors, such as smaller bleaching events, diseases, and possibly illegal fishing, among other environmental complexities that were not studied and modeled.

These results and modest fit to field empirical data were supported by values for ecological ratios that are consistent with those reported in the literature. This is encouraging given that, in contrast to other commonly-used trophodynamic models (e.g. EwE), these outputs are emergent in CAFFEE rather than input forcing values; they result from the approach of linking biomass-density based benthic production with reef cover dynamics. CAFFEE is also fully coupled, bringing together difficult-to-quantify aspects of the detrital and calcium carbonate linkages that can be so critical to evaluating the fate of production processes. They also greatly influence soft-bottom (seagrass) and pelagic systems that are not typically modeled for coral reefs; yet are critical to fisheries and other ecosystem services (McClanahan et al., 2008). These characteristics situate the CAFFEE modeling approach in line with current efforts to develop end-to-end models (Travers et al., 2007). However, the integration of physical, biological and ecological processes in CAFFEE comes at the cost of model assumptions and extensive parameterization sets, for which (in some cases), there may be little or no empirical support. Future uses of this model will evaluate the model's ability to predict and project fisheries and other types of management based on this energy and materials-based view of the ecosystem.

Acknowledgements

The support of the John D. and Catherine T. MacArthur Foundation and Western Indian Ocean Marine Science Association – Marine Science for Management (WIOMSA-MASMA) program are greatly appreciated. M. Ateweberhan, A. Baker, H. Bruggemann, J. Cinner, N. Graham, M. Guillaume, A. Halford, J. Maina, A. MacNeil, J. Mate, C. Muhando, M. Suleiman, A. Ussi, S. Wilson and S. Yahya helped with the conceptualization of early versions of the food web. We thank 2 anonymous reviewers for their constructive comments.

Appendix A. Supplementary data

Supplementary data associated with this article can be found, in the online version, at http://dx.doi.org/10.1016/j.ecolmodel.2013.05.012.

References

Abdullah, M.I., Fredriksen, S., 2004. Production, respiration and exudation of dissolved organic matter by the kelp *Laminaria hyperborea* along the west coast of Norway. Journal of the Marine Biological Association of the UK 84, 887–894.
Abrams, P.A., Ginzburg, L.R., 2000. The nature of predation: prey dependent, ratio dependent or neither? Trends in Ecology & Evolution 15, 337–341.
Akçakaya, H.R., Arditi, R., Ginzburg, L.R., 1995. Ratio-dependent predation: an abstraction that works. Ecology 76, 995–1004.
Aljetlawi, A.A., Sparrevik, E., Leonardsson, K., 2004. Prey–predator size-dependent functional response: derivation and rescaling to the real world. Journal of Animal Ecology 73, 239–252.
Alwany, M.A., Thaler, E., Stachowitsch, M., 2009. Parrotfish bioerosion on Egyptian Red Sea reefs. Journal of Experimental Marine Biology and Ecology 371, 170–176.
Amon, R.M.W., Benner, R., 1996. Bacterial utilization of different size classes of dissolved organic matter. Limnology & Oceanography 41, 41–51.
Anthony, K.R.N., Fabricius, K.E., 2000. Shifting roles of heterotrophy and autotrophy in coral energetics under varying turbidity. Journal of Experimental Marine Biology and Ecology 252, 221–253.
Anthony, K.R.N., Connolly, S.R., Willis, B.L., 2002. Comparative analysis of energy allocation to tissue and skeletal growth in corals. Limnology & Oceanography 47, 1417–1429.
Anthony, K.R.N., Connolly, S.R., 2004. Environmental limits to growth: physiological niche boundaries of corals along turbidity–light gradients. Oecologia 141, 373–384.
Arditi, R., Ginzburg, L.R., 1989. Coupling in predator–prey dynamics: ratio-dependence. Journal of Theoretical Biology 139, 311–326.
Arditi, R., Saïah, H., 1992. Empirical evidence of the role of heterogeneity in ratio-dependent consumption. Ecology 73, 1544–1551.
Arias-González, J.E., 1998. Trophic models of protected and unprotected coral reef ecosystems in the south of the Mexican Caribbean. Journal of Fish Biology 53, 236–255.
Arias-González, J.E., Nuñez-Lara, E., González-Salas, C., Galzin, R., 2004. Trophic models for investigation of fishing effect on coral reef ecosystems. Ecological Modelling 172, 197–212.
Ateweberhan, M., Bruggemann, J.H., Breeman, A.M., 2006. Effects of extreme seasonality on community structure and functional group dynamics of coral reef algae in the southern Red Sea (Eritrea). Coral Reefs 25, 391–406.
Bandeira, S.O., 2002. Leaf production rates of *Thalassodendron ciliatum* from rocky and sandy habitats. Aquatic Botany 72, 13–24.
Baskett, M.L., Gaines, S.D., Nisbet, R.M., 2009. Symbiont diversity may help coral reefs survive moderate climate change. Ecological Applications 19, 3–17.
Baskett, M.L., Nisbet, R.M., Kappel, C.V., Mumby, P.J., Gaines, S.D., 2010. Conservation management approaches to protecting the capacity for corals to respond to climate change: a theoretical comparison. Global Change Biology 16, 1229–1246.
Bellwood, D.R., 1995. Carbonate transport and within-reef patterns of bioerosion and sediment release by parrotfishes (family Scaridae) on the Great Barrier Reef. Marine Ecology Progress Series 117, 127–136.
Bellwood, D.R., Hoey, A.S., Hughes, T.P., 2012. Human activity selectively impacts the ecosystem roles of parrotfishes on coral reefs. Proceedings of the Royal Society B 279, 1621–1629.
Berryman, A.A., 1992. The origins and evolution of predator–prey theory. Ecology 73, 1530–1535.
Berryman, A.A., Gutierrez, A.P., Arditi, R., 1995. Credible, parsimonious and useful predator–prey models: a reply to Abrams, Gleeson, and Sarnelle. Ecology 76, 1980–1985.
Berumen, M.L., Pratchett, M.S., McCormick, M.I., 2005. Within-reef differences in diet and body condition of coral-feeding butterflyfishes (Chaetodontidae). Marine Ecology Progress Series 287, 217–227.
Berumen, M.L., Pratchett, M.S., 2008. Trade-offs associated with dietary specialization in corallivorous butterflyfishes (Chaetodontidae: Chaetodon). Behavioral Ecology and Sociobiology 62, 989–994.

Boisclair, D., 2001. Fish habitat modeling: from conceptual framework to functional tools. Canadian Journal of Fisheries and Aquatic Sciences 58, 1–9.
Boisclair, D., Legget, W.C., 1989. The importance of activity in bioenergetics models applied to actively foraging fishes. Canadian Journal of Fisheries and Aquatic Sciences 46, 1859–1867.
Bourne, D., Iida, Y., Uthicke, S., Smith-Keyne, C., 2008. Changes in coral-associated microbial communities during a bleaching event. ISME Journal 2, 350–363.
Bozec, Y.M., Gascuel, D., Kulbicki, M., 2004. Trophic model of lagoonal communities in a large open atoll (Uvea, Loyalty islands, New Caledonia). Aquatic Living Resources 17, 151–162.
Brown-Saracino, J., Peckol, P., Curran, H.A., Robbart, M.L., 2007. Spatial variation in sea urchins, fish predators, and bioerosion rates on coral reefs of Belize. Coral Reefs 26, 71–78.
Bruggemann, J.H., van Kessel, A.M., van Rooij, J.M., Breeman, A.M., 1996. Bioerosion and sediment ingestion by the Caribbean parrotfish *Scarus vetula* and *Sparisoma viride*: implications of fish size, feeding mode and habitat use. Marine Ecology Progress Series 134, 59–71.
Carpenter, R.C., 1985. Relationships between primary production and irradiance in coral reef algal communities. Limnology & Oceanography 30, 784–793.
Carpenter, S.R., Cottingham, K.L., Stow, C.A., 1994. Fitting predator–prey models to time series with observation errors. Ecology 75, 1254–1264.
Carreiro-Silva, M., McClanahan, T.R., 2001. Echinoid bioerosion and herbivory on Kenyan coral reefs: the role of protection from fishing. Journal of Experimental Marine Biology and Ecology 262, 133–153.
Carricart-Ganivet, J.P., Beltrán-Torres, A.U., Merino, M., Ruiz-Zárate, M.A., 2008. Skeletal extension, density and calcification rate of the reef-building coral Montastrea annularis (Ellis and Solander) in the Mexican Caribbean. Bulletin of Marine Science 66, 215–224.
Chipps, S.R., Wahl, D.H., 2008. Bioenergetics modeling in the 21st century: reviewing new insights and revisiting old constraints. Transactions of the American Fisheries Society 137, 298–313.
Chisholm, J.R.M., 2003. Primary productivity of reef-building crustose coralline algae. Limnology & Oceanography 48, 1376–1387.
Chong-Seng, K., Mannering, T.D., Pratchett, M.S., Bellwood, D.R., Graham, N.A.J., 2012. The influence of coral reef benthic condition on associated fish assemblages. PLOS One 7, e42167.
Cinner, J.E., McClanahan, T.R., Graham, N.A.J., Pratchett, M.S., Wilson, S.K., Raina, J.B., 2009. Gear-based fisheries management as a potential adaptive response to climate change and coral mortality. Journal of Applied Ecology 46, 724–732.
Coffroth, M.A., 1990. Mucous sheet formation on poritid corals: an evaluation of coral mucus as a nutrient source on reefs. Marine Biology 105, 39–49.
Cole, A.J., Pratchett, M.S., Jones, G.P., 2008. Diversity and functional importance of coral-feeding fishes on tropical coral reefs. Fish Fish 9, 286–307.
Connell, J.H., Hughes, T.P., Wallace, C.C., 1997. A 30-year study of coral abundance, recruitment, and disturbance at several scales in space and time. Ecological Monographs 67, 461–488.
Copertino, M., Connell, S.D., Cheshire, A., 2005. The prevalence and production of turf-forming algae on a temperate subtidal coast. Phycologia 44, 241–248.
Copertino, M.S., Cheshire, A., Kildea, T., 2009. Photophysiology of a turf algal community: integrated responses to ambient light and standing biomass. Journal of Phycology 45, 324–336.
Crabbe, M.J.C., 2008. Climate change, global warming and coral reefs: modelling the effects of temperature. Computational Biology and Chemistry 32, 311–314.
Crossland, C.J., 1987. In situ release of mucus and DOC-lipid from the corals *Acropora variabilis* and *Stylophora pistillata* in different light regimes. Coral Reefs 6, 35–42.
Davies, P.J., 1983. Reef growth. In: Barnes, D.J. (Ed.), Perspectives on Coral Reefs. Australian Institute of Marine Science, Manuka, pp. 69–106.
DeMartini, E.E., Friedlander, A.M., Sandin, S.A., Sala, E., 2008. Differences in fish-assemblage structure between fished and unfished atolls in the northern Line Islands, central Pacific. Marine Ecology Progress Series 365, 199–215.
de Villemereuil, P.B., López-Sepulcre, A., 2011. Consumer functional responses under intra- and inter-specific interference competition. Ecological Modelling 222, 419–426.
Dhargalkar, V.K., Shaikh, N., 2000. Primary productivity of marine macrophytes in the coral reef lagoon of the Kadmat Island, Lakshadweep. Current Science (India) 79, 1101–1104.
Duarte, C.M., Chiscano, C.L., 1999. Seagrass biomass and production: a reassessment. Aquatic Botany 65, 159–174.
Eggleston, D.B., Lipcius, R.N., Hines, A.H., 1992. Density-dependent predation by blue crabs upon infaunal clam species with contrasting distribution and abundance patterns. Marine Ecology Progress Series 85, 55–68.
Englund, G., Leonardsson, K., 2008. Scaling up the functional response for spatially heterogeneous systems. Ecology Letters 11, 440–449.
Falkowski, P.G., Dubinsky, Z., Muscatine, L., Porter, J.W., 1984. Light and the bioenergetics of a symbiotic coral. Bioscience 34, 705–709.
Ferrier-Pagès, C., Gattuso, J.P., 1998. Biomass, production and grazing rates of pico- and nanoplankton in coral reef waters (Miyako Island, Japan). Microbial Ecology 35, 46–57.
Ferrier-Pagès, C., Witting, J., Tambutté, E., Sebens, K.P., 2003. Effect of natural zooplankton feeding on the tissue and skeletal growth of the scleractinian coral *Stylophora pistillata*. Coral Reefs 22, 229–240.
Fitt, W.K., McFarland, F.K., Warner, M.E., Chilcoat, G.C., 2000. Seasonal patterns of tissue biomass and densities of symbiotic dinoflagellates in reef corals and relation to coral bleaching. Limnology & Oceanography 45, 677–685.
Gamble, R.J., Link, J.S., 2009. Analyzing the tradeoffs among ecological and fishing effects on an example fish community: a multispecies (fisheries) production model. Ecological Modelling 220, 2570–2582.
Garpe, K.C., Öhman, M.C., 2003. Coral and fish distribution patterns in Mafia Island Marine Park, Tanzania: fish–habitat interactions. Hydrobiologia 498, 191–211.
Garrigue, C., 1991. Biomass and production of two Halimeda species in the Southwest New Caledonian lagoon. Oceanologica Acta 14, 581–588.
Gilmour, J.P., Smith, L.D., Heyward, A.J., Baird, A.H., Pratchett, M.S., 2013. Recovery of an isolated coral reef system following severe disturbance. Science 340, 69–71.
Ginzburg, L.R., Akçakaya, H.R., 1992. Consequences of ratio-dependent predation for steady-state properties of ecosystems. Ecology 73, 1536–1543.
Glynn, P.W., 1996. Bioerosion and coral reef growth. In: Birkeland, C. (Ed.), Life and Death of Coral Reefs. Chapman & Hall, New York, pp. 69–98.
Gochfeld, D.J., 1991. Energetics of a predator–prey interaction: corals and coral-feeding fishes. Pacific Science 45, 246–256.
Graham, N.A.J., 2007. Ecological versatility and the decline of coral feeding fishes following climate driven coral mortality. Marine Biology 153, 119–127.
Graham, N.A.J., McClanahan, T.R., MacNeil, M.A., Wilson, S.K., Polunin, N.V.C., Jennings, S., et al., 2008. Climate warming, marine protected areas and the ocean-scale integrity of coral reef ecosystems. PLOS One 3, e3039.
Graham, N.A.J., Chabanet, P., Evans, R.D., Jennings, S., Letourneur, Y., MacNeil, M.A., et al., 2011. Extinction vulnerability of coral reef fishes. Ecology Letters 14, 341–348.
Grottoli, A.G., Rodrigues, L.J., Palardy, J.E., 2006. Heterotrophic plasticity and resilience in bleached corals. Nature 440, 1186–1189.
Haapkylä, J., Unsworth, R.K.F., Flavell, M., Bourne, D.G., Schaffelke, B., Willis, B.L., 2011. Seasonal rainfall and runoff promote coral disease on an inshore reef. PLOS One 6, 443–449.
Haas, A., Al-Zibdah, M., Wild, C., 2009. Effect of inorganic and organic nutrient addition on coral–algae assemblages from the Northern Red Sea. Journal of Experimental Marine Biology and Ecology 380, 99–105.
Haas, A.F., Nelson, C.E., Wegley, K.L., Carlson, C.A., Rohwer, F., Leichter, J.J., et al., 2011. Effects of coral reef benthic primary producers on dissolved organic carbon and microbial activity. PLOS One 6, e27973.
Hackney, J.M., Sze, P., 1988. Photorespiration and productivity rates of a coral reef algal turf assemblage. Marine Biology 98, 483–492.
Hay, M.E., 1996. Marine chemical ecology: what's known and what's next? Journal of Experimental Marine Biology and Ecology 200, 103–134.
Heck Jr., K.L., Carruthers, T.J.B., Duarte, C.M., Hughes, A.R., Kendrick, G., Orth, R.J., et al., 2008. Trophic transfers from seagrass meadows subsidize diverse marine and terrestrial consumers. Ecosystems 11, 1198–1210.
Hoey, A.S., Bellwood, D.R., 2008. Cross-shelf variation in the role of parrotfishes on the Great Barrier Reef. Coral Reefs 27, 37–47.
Holmes, G., 2008. Estimating three-dimensional surface areas on coral reefs. Journal of Experimental Marine Biology and Ecology 365, 67–73.
Holmes, G., Johnstone, R.W., 2010. Modelling coral reef ecosystems with limited observational data. Ecological Modelling 221, 1173–1183.
Houlbrèque, F., Tambutté, E., Allemand, D., Ferrier-Pagès, C., 2004. Interactions between zooplankton feeding, photosynthesis and skeletal growth in the scleractinian coral *Stylophora pistillata*. Journal of Experimental Biology 207, 1461–1469.
Houlbrèque, F., Ferrier-Pagès, C., 2009. Heterotrophy in tropical scleractinian corals. Biological Reviews 84, 1–17.
Hughes, T.P., 1987. Skeletal density and growth form of corals. Marine Ecology Progress Series 35, 259–266.
Jayewardene, D., Birkeland, C., 2006. Fish predation on Hawaiian corals. Coral Reefs 25, 328.
Jayewardene, D., Donahue, M.J., Birkeland, C., 2009. Effects of frequent fish predation on corals in Hawaii. Coral Reefs 28, 499–506.
Jiddawi, N.S., Öhman, M.C., 2002. Marine fisheries in Tanzania. Ambio 31, 518–527.
Kayanne, H., Hata, H., Kudo, S., Yamano, H., Watanabe, A., Ikeda, Y., et al., 2005. Seasonal and bleaching-induced changes in coral reef metabolism and CO_2 flux. Global Biogeochemical Cycles 19, 1–11.
Khailov, K.M., Burlakova, Z.P., 1969. Release of dissolved organic matter by marine seaweeds and distribution of their total organic production to inshore communities. Limnology & Oceanography 14, 521–527.
Kim, K., Lasker, H.R., 1998. Allometry of resource capture in colonial cnidarians and constraints on modular growth. Functional Ecology 12, 646–654.
Kirsch, K.D., Valentine, J.F., Heck, K.L., 2002. Parrotfish grazing on turtlegrass *Thalassia testudinum*: evidence for the importance of seagrass consumption in food web dynamics of the Florida Keys National Marine Sanctuary. Marine Ecology Progress Series 227, 71–85.
Langmead, O., Sheppard, C., 2004. Coral reef community dynamics and disturbance: a simulation model. Ecological Modelling 175, 271–290.
Ledlie, M.H., Graham, N.A.J., Bythell, J.C., Wilson, S.K., Jennings, S., Polunin, N.V.C., et al., 2007. Phase shifts and the role of herbivory in the resilience of coral reefs. Coral Reefs 26, 641–653.
Lirman, D., 2001. Competition between macroalgae and corals: effects of herbivore exclusion and increased algal biomass on coral survivorship and growth. Coral Reefs 19, 392–399.
Littler, M.M., Kauker, B.J., 1984. Heterotrichy and survival strategies in the red alga *Corallina officinalis* L. Botanica Marina 27, 37–44.
Littler, M.M., Littler, D.S., Blair, S.M., Norris, J.N., 1986. Deep-water plant communities from an uncharted seamount off San Salvador Island, Bahamas: distribution, abundance and primary productivity. Deep-Sea Research 33, 881–892.

Littler, M.M., Littler, D.S., Taylor, P.R., 1995. Selective herbivore increases biomass of its prey: a chiton-coralline reef-building association. Ecology 76, 1666–1681.
Liu, P.J., Shao, K.T., Jan, R.Q., Fan, T.Y., Wong, S.L., Hwang, J.S., et al., 2009. A trophic model of fringing coral reefs in Nanwan Bay, southern Taiwan suggests overfishing. Marine Environmental Research 68, 106–117.
Mallela, J., 2007. Coral reef encruster communities and carbonate production in cryptic and exposed coral reef habitats along a gradient of terrestrial disturbance. Coral Reefs 26, 775–785.
Marsh Jr., J.A., 1970. Primary productivity of reef-building calcareous red algae. Ecology 51, 255–263.
Martin, S., Castets, M.D., Clavier, J., 2006. Primary production, respiration and calcification of the temperate free-living coralline alga *Lithothamnion corallioides*. Aquatic Botany 85, 121–128.
McClanahan, T.R., 1992. Resource utilization, competition, and predation: a model and example from coral reef grazers. Ecological Modelling 61, 195–215.
McClanahan, T.R., 1994. Kenyan coral reef lagoon fish: effects of fishing, substrate complexity, and sea urchins. Coral Reefs 13, 231–241.
McClanahan, T.R., 1995. A coral reef ecosystem-fisheries model: impacts of fishing intensity and catch selection on reef structure and processes. Ecological Modelling 80, 1–19.
McClanahan, T.R., 1997. Primary succession of coral-reef algae: differing patterns on fished versus unfished reefs. Journal of Experimental Marine Biology and Ecology 218, 77–102.
McClanahan, T.R., 2008. Response of the coral reef benthos and herbivory to fishery closure management and the 1998 ENSO disturbance. Oecologia 155, 169–177.
McClanahan, T.R., 2013. How long for recovery and reversal of trophic cascades in tropical coral reef fisheries closures? Conservation Biology (in review).
McClanahan, T., Maina, J., Pet-Soede, L., 2002a. Effects of the 1998 coral mortality event on Kenyan coral reefs and fisheries. AMBIO 31, 7–8.
McClanahan, T.R., Muthiga, N.A., Mangi, S., 2001. Coral and algal changes after the 1998 coral bleaching: interaction with reef management and herbivores on Kenyan reefs. Coral Reefs 19, 380–391.
McClanahan, T.R., Polunin, N., Done, T., 2002b. Ecological states and the resilience of coral reefs. Conservation Ecology 6, 18–45.
McClanahan, T.R., McLaughlin, S.M., Davy, J.E., Wilson, W.H., Peters, E.C., Price, K.L., et al., 2004. Observations of a new source of coral mortality along the Kenyan coast. Hydrobiologia 530/531, 469–479.
McClanahan, T.C., Maina, J., Starger, C.J., Herron-Perez, P., Dusek, E., 2005. Detriments to post-bleaching recovery of corals. Coral Reefs 24, 230–246.
McClanahan, T.R., Hicks, C.C., Darling, E.S., 2008. Malthusian overfishing and efforts to overcome it on Kenyan coral reefs. Ecological Applications 18, 1516–1529.
McClanahan, T.R., Shafir, S.H., 1990. Causes and consequences of sea urchin abundance and diversity in Kenyan coral reef lagoons. Oecologia 83, 362–370.
McClanahan, T.R., Graham, N.A.J., 2005. Recovery trajectories of coral reef fish assemblages within Kenyan marine protected areas. Marine Ecology Progress Series 294, 241–248.
McCloskey, L.R., Muscatine, L., 1984. Production and respiration in the Red Sea coral *Stylophora pistillata* as a function of depth. Proceedings of the Royal Society B 222, 215–230.
Meesters, E.H., Bak, R.P.M., Westmacott, S., Ridgley, M., Dollar, S., 1998. A fuzzy logic model to predict coral reef development under nutrient and sediment stress. Conservation Biology 12, 957–965.
Miller, R.J., Reed, D.C., Brzezinski, M.A., 2009. Community structure and productivity of subtidal turf and foliose algal assemblages. Marine Ecology Progress Series 388, 1–11.
Mumby, P.F., Hedley, J.D., Zychaluk, K., Harborne, A.R., Blackwell, P.G., 2006. Revisiting the catastrophic die-off of the urchin *Diadema antillarum* on Caribbean coral reefs: fresh insights on resilience from a simulation model. Ecological Modelling 196, 131–148.
Mumby, P.J., Hastings, A., Edwards, H.J., 2007. Thresholds and the resilience of Caribbean coral reefs. Nature 450, 98–101.
Mumby, P.J., 2009a. Herbivory versus corallivory: are parrotfish good or bad for Caribbean coral reefs? Coral Reefs 28, 683–690.
Mumby, P.J., 2009b. Phase shifts and the stability of macroalgal communities on Caribbean coral reefs. Coral Reefs 28, 761–773.
Muscatine, L., Falkowski, P.G., Porter, J.W., Dubinsky, Z., 1984. Fate of photosynthetic fixed carbon in light- and shade-adapted colonies of the symbiotic coral *Stylophora pistillata*. Proceedings of the Royal Society B 222, 181–202.
Mutua, A.K., Mavuti, K.M., Daro, N., Tackx, M., 2004. Spatial distribution of suspended particulate matter in Mtwapa Creek and Funzi Bay, Kenya. Western Indian Ocean Journal of Marine Science 3, 29–36.
Nakajima, R., Yoshida, T., Azman, B.A.R., Zaleha, K., Othman, B.H.R., Toda, T., 2009. In situ release of coral mucus by Acropora and its influence on the heterotrophic bacteria. Aquatic Ecology 43, 815–823.
Nakajima, R., Yoshida, T., Fujita, K., Nakayama, A., Fuchinoue, Y., Othman, B.H.R., et al., 2010. Release of particulate and dissolved organic carbon by the scleractinian coral *Acropora formosa*. Bulletin of Marine Science 86, 861–870.
Nugues, M.M., Smith, G.W., van Hooidonk, R.J., Seabra, M.I., Bak, R.P.M., 2004. Algal contact as a trigger for coral disease. Ecology Letters 7, 919–923.
Ochieng, C.A., Erftemeijer, P.L.A., 1999. Accumulation of seagrass beach cast along the Kenyan coast: a quantitative assessment. Aquatic Botany 65, 221–238.
O'Leary, J.K., McClanahan, T.R., 2010. Trophic cascades result in large-scale coralline algae loss through differential grazer effects. Ecology 91, 3584–3597.
O'Leary, J.K., Potts, D.C., Braga, J.C., McClanahan, T.R., 2012. Indirect consequences of fishing: reduction of coralline algae suppresses juvenile coral abundance. Coral Reefs 31, 547–559.
Opitz, S., 1996. Trophic interactions in Caribbean coral reefs. ICLARM Technical Report 43. ICLARM, Manila.
Paine, R.T., Vadas, R.L., 1969. Calorific values of benthic marine algae and their postulated relation to invertebrate food preference. Marine Biology 4, 79–86.
Palardy, J.E., Grottoli, A.G., Matthews, K.A., 2006. Effect of naturally changing zooplankton concentrations on feeding rates of two coral species in the Eastern Pacific. Journal of Experimental Marine Biology and Ecology 331, 99–107.
Palardy, J.E., Rodrigues, L.J., Grottoli, A.G., 2008. The importance of zooplankton to the daily metabolic carbon requirements of healthy and bleached corals at two depths. Journal of Experimental Marine Biology and Ecology 367, 180–188.
Pandolfi, J.M., Connolly, S.R., Marshall, D.J., Cohen, A.L., 2011. Projecting coral reef futures under global warming and ocean acidification. Science 333, 418–422.
Pausz, C., Herndl, G.J., 1999. Role of ultraviolet radiation on phytoplankton extracellular release and its subsequent utilization by marine bacterioplankton. Aquatic Microbial Ecology 18, 85–93.
Penhale, P.A., Capone, D.G., 1981. Primary productivity and nitrogen fixation in two macroalgae-cyanobacteria associations. Bulletin of Marine Science 31, 164–169.
Perry, C., Edinger, E., Kench, P., Murphy, G., Smithers, S., Steneck, R., et al., 2012. Estimating rates of biologically driven coral reef framework production and erosion: a new census-based carbonate budget methodology and applications to the reefs of Bonaire. Coral Reefs 31, 853–868.
Pett, R.J., 1989. Kinetics of microbial mineralization of organic carbon from detrital *Skeletonema costatum* cells. Marine Ecology Progress Series 52, 123–128.
Piana, P.A., Gomes, L.C., Agostinho, A.A., 2006. Comparison of predator–prey interaction models for fish assemblages from the neotropical region. Ecological Modelling 192, 259–270.
Pistorius, P.A., Taylor, F.E., 2009. Declining catch rates of reef fish in Aldabra's marine protected area. Aquatic Conservation 19, s2–s9.
Polovina, J.J., 1984. Model of a coral reef ecosystem. I. The ECOPATH model and its application to French Frigate shoals. Coral Reefs 3, 1–11.
Pomeroy, L.R., Sheldon, J.E., Sheldon Jr., W.M., Peters, F., 1995. Limits to growth and respiration of bacterioplankton in the Gulf of Mexico. Marine Ecology Progress Series 117, 259–268.
Porter, J.W., Muscatine, L., Dubinsky, Z., Falkowski, P.G., 1984. Primary production and photoadaptation in light- and shade-adapted colonies of the symbiotic coral, *Stylophora pistillata*. Proceedings of the Royal Society B 222, 161–180.
Pratchett, M.S., Wilson, S.K., Baird, A.H., 2006. Declines in the abundance of Chaetodon butterflyfishes following extensive coral depletion. Journal of Fish Biology 69, 1269–1280.
Pratchett, M.S., Munday, P.L., Wilson, S.K., Graham, N.A.J., Cinner, J.E., Bellwood, D.R., et al., 2008. Effects of climate-induced coral bleaching on coral-reef fishes – ecological and economic consequences. Oceanography and Marine Biology 46, 251–296.
Riegl, B., Branch, G.M., 1995. Effects of sediment on the energy budgets of four scleractinian (Bourne 1900) and five alcyonacean (Lamouroux 1816) corals. Journal of Experimental Marine Biology and Ecology 186, 259–275.
Robertson, D.R., 1987. Responses of two coral reef toadfishes (Batrachoididae) to the demise of their primary prey, the sea urchin *Diadema antillarum*. Copeia 3, 637–642.
Robertson, D.R., 1991. Increases in surgeonfish populations after mass mortality of the sea urchin *Diadema antillarum* in Panama indicate food limitation. Marine Biology 111, 437–444.
Rogers, C.S., Salesky, H., 1981. Productivity of *Acropora palmata* (Lamarck), macroscopic algae, and algal turf from Tague Bay reef, St. Croix, US Virgin Islands. Journal of Experimental Marine Biology and Ecology 49, 179–187.
Russ, G.A., Alcala, A.C., 2004. Marine reserves: long-term protection is required for full recovery of predatory fish populations. Oecologia 138, 622–627.
Sandin, S.A., Smith, J.E., DeMartini, E.E., Dinsdale, E.A., Donner, S.D., Friedlander, A.M., et al., 2008. Baselines and degradation of coral reefs in the Northern Line islands. PLOS One 3, e1548.
Schenk, D., Bersier, L.F., Bacher, S., 2005. An experimental test of the nature of predation: neither prey- nor ratio-dependent. Journal of Animal Ecology 74, 86–91.
Sogard, S.M., Olla, B.L., 1996. Food deprivation affects vertical distribution and activity of a marine fish in a thermal gradient: potential energy-conserving mechanisms. Marine Ecology Progress Series 133, 43–55.
Sorokin, Y.I., 1982. Aspects of the biomass, feeding and metabolism of common corals of the Great Barrier Reef, Australia. In: Gomez, E.D., Birkeland, C.E., Buddemeier, R.W., Johannes, R.E., Marsh, J.A., Tsuda, R.T. (Eds.), Proceedings of the 4th International Coral Reef Symposium. University of the Philippines, Manila, pp. 27–32.
Sorokin, Y.I., Sorokin, P.Y., 2009. Analysis of plankton in the southern Great Barrier Reef: abundance and roles in trophodynamics. Journal of the Marine Biological Association of the UK 89, 235–241.
Tanaka, Y., Miyajima, T., Koike, I., Hayashibara, T., Ogawa, H., 2008. Production of dissolved and particulate organic matter by the reef-building corals *Porites cylindrica* and *Acropora pulchra*. Bulletin of Marine Science 82, 237–245.
Tranvik, L., Kokalj, S., 1998. Decreased biodegradability of algal DOC due to interactive effects of UV radiation and humic matter. Aquatic Microbial Ecology 14, 301–307.
Travers, M., Shin, Y.J., Jennings, S., Cury, P., 2007. Towards end-to-end models for investigating the effects of climate and fishing in marine ecosystems. Progress in Oceanography 75, 751–770.
Tudman, P.D., 2001. Modelling the Trophic Effects of Fishing on a Midshelf Coral Reef of the Central Great Barrier Reef. James Cook University, Townsville.
van der Elst, R., Everett, B., Jiddawi, N., Mwatha, G., Santana, A.P., Boulle, D., 2005. Fish, fishers and fisheries of the Western Indian Ocean: their diversity and status.

A preliminary assessment. Philosophical Transactions of the Royal Society A 363, 263–284.
van Tussenbroek, B.I., 1998. Above- and below-ground biomass and production by *Thalassia testudinum* in a tropical reef lagoon. Aquatic Botany 61, 69–82.
van Woesik, R., Sakai, K., Ganase, A., Loya, Y., 2011. Revisiting the winners and loser a decade after coral bleaching. Marine Ecology Progress Series 434, 67–76.
Villinski, J.T., 2003. Depth-independent reproductive characteristics for the Caribbean reef-building coral *Montastraea faveolata*. Marine Biology 142, 1043–1053.
Viherluoto, M., Viitasalo, M., 2001. Temporal variability in functional responses and prey selectivity of the pelagic mysid, *Mysis mixta*, in natural prey assemblages. Marine Biology 138, 575–583.
Wada, S., Aoki, M.N., Tsuchiya, Y., Sato, T., Shinagawa, H., Hama, T., 2007. Quantitative and qualitative analyses of dissolved organic matter released from Ecklonia cava Kjellman, in Oura Bay, Shimoda, Izu Peninsula, Japan. Journal of Experimental Marine Biology and Ecology 349, 344–358.
Wada, S., Aoki, M.N., Mikami, A., Komatsu, T., Tsuchiya, Y., Sato, T., et al., 2008. Bioavailability of macroalgal dissolved organic matter in seawater. Marine Ecology Progress Series 370, 33–44.
Wanders, J.B.W., 1976a. The role of benthic algae in the shallow reef of Curaçao (Netherlands antilles) I: primary productivity in the coral reef. Aquatic Botany 2, 235–270.
Wanders, J.B.W., 1976b. The role of benthic algae in the shallow reef of Curaçao (Netherlands antilles) II: primary productivity of the Sargassum beds on the north-east coast submarine plateau. Aquatic Botany 2, 327–335.
Wild, C., Huettel, M., Klueter, A., Kremb, S.G., Rasheed, M.Y.M., Jørgensen, B.B., 2004. Coral mucus functions as an energy carrier and particle trap in the reef ecosystem. Nature 428, 66–70.
Wilson, S.K., Graham, N.A.J., Pratchett, M.S., Jones, G.P., Polunin, N.V.C., 2006. Multiple disturbances and the global degradation of coral reefs: are reef fishes at risk or resilient? Global Change Biology 12, 2220–2234.
Wolanski, E., Richmond, R.H., McCook, L., 2004. A model of the effects of land-based, human activities on the health of coral reefs in the Great Barrier Reef and in Fouha Bay, Guam, Micronesia. Journal of Marine Systems 46, 133–144.
Ziegler, S., Benner, R., 1999. Dissolved organic carbon cycling in a subtropical seagrass-dominated lagoon. Marine Ecology Progress Series 180, 149–160.